Journal Pre-proofs

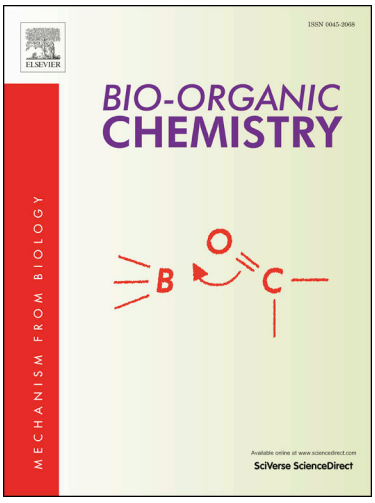

Design and Synthesis of Novel quinoline/chalcone/1,2,4-triazole hybrids as potent antiproliferative agent targeting EGFR and $BRAF^{V600E}$ kinases

Aliaa M. Mohassab, Heba A. Hassan, Dalia Abdelhamid, Ahmed M. Gouda, Bahaa G. M. Youssif, Hiroshi Tateishi, Mikako Fujita, Masami Otsuka, Mohamed Abdel-Aziz

PII: S0045-2068(20)31808-3
DOI: https://doi.org/10.1016/j.bioorg.2020.104510
Reference: YBIOO 104510

To appear in: *Bioorganic Chemistry*

Received Date: 15 June 2020
Revised Date: 10 October 2020
Accepted Date: 19 November 2020

Please cite this article as: A.M. Mohassab, H.A. Hassan, D. Abdelhamid, A.M. Gouda, B. G. M. Youssif, H. Tateishi, M. Fujita, M. Otsuka, M. Abdel-Aziz, Design and Synthesis of Novel quinoline/chalcone/1,2,4-triazole hybrids as potent antiproliferative agent targeting EGFR and $BRAF^{V600E}$ kinases, *Bioorganic Chemistry* (2020), doi: https://doi.org/10.1016/j.bioorg.2020.104510

Design and Synthesis of Novel quinoline/chalcone/1,2,4-triazole hybrids as potent antiproliferative agent targeting EGFR and BRAF^{V600E} kinases

Aliaa M. Mohassab [a], Heba A. Hassan [a]*, Dalia Abdelhamid [a], Ahmed M. Gouda [b], Bahaa G. M. Youssif [c*], Hiroshi Tateishi [d], Mikako Fujita [d], Masami Otsuka [d,e], Mohamed Abdel-Aziz[a]

[a] Department of Medicinal Chemistry, Faculty of Pharmacy, Minia University, Minia 61519, Egypt, [b]Department of Medicinal Chemistry, Faculty of Pharmacy, Beni-Suef University, Beni-Suef 62514, Egypt, [C] Pharmaceutical Organic Chemistry Department, Faculty of Pharmacy, Assiut University, Assiut 71526, Egypt., [d] Medicinal and Biological Chemistry Science Farm Joint Research Laboratory, Faculty of Life Sciences, Kumamoto University, 5-1 Oe-honmachi, Chuo-ku, Kumamoto, Kumamoto 862-0973, Japan., [e] Department of Drug Discovery, Science Farm Ltd., 1-7-30 Kuhonji, Chuo-ku, Kumamoto, Kumamoto 862-0976, Japan.

Short running title: Synthesis and antiproliferative activity of new quinoline/chalcone/1,2,4-triazole hybrid.

**To whom correspondence should be addressed:*

Mohamed Abdel-Aziz, Ph.D. Department of Medicinal Chemistry, Faculty of Pharmacy, Minia University, 61519-Minia, Egypt.

Tel.:(002)-01003311327

E-mail address: Abulnil@hotmail.com

Heba A. Hassan, Ph.D. Department of Medicinal Chemistry, Faculty of Pharmacy, Minia University, 61519-Minia, Egypt.

Tel.:(002)-01068390918

E-mail address: heba.hasan@mu.edu.eg

Bahaa G. M. Youssif, Ph.D. Pharmaceutical Organic Chemistry Department, Faculty of Pharmacy, Assiut University, Assiut 71526, Egypt.

Tel.: (002)-01098294419

E-mail address: bgyoussif@ju.edu.sa, bahaa.youssif@pharm.aun.edu.eg

Abstract

New quinoline / chalcone hybrids containing 1,2,4-triazole moiety have been designed, synthesized and their structures elucidated and confirmed by various spectroscopic techniques. The designed compounds showed moderate to good activity on different NCI 60 cell lines in a single-dose assay with a growth inhibition rate ranging from 50% to 94%. Compounds **7b**, **7d**, **9b**, and **9d** were the most active compounds in most cancer cell lines with a growth inhibition percent between 77% and 94%. Newly synthesized hybrids were evaluated for their anti-proliferative activity against a panel of four human cancer cell lines. Compounds **7a, 7b, 9a, 9b,** and **9d** showed promising antiproliferative activities. These compounds were further tested for their inhibitory potency against EGFR and $BRAF^{V600E}$ kinases with erlotinib as a reference drug. The molecular docking study of compounds **7a, 7b, 9a, 9b,** and **9d** revealed nice fitting into the active site of EGFR and $BRAF^{V600E}$ kinases. Compounds **7b**, **9b**, and **9d** displayed the highest binding affinities and similar binding pattern to those of erlotinib.

Key words: Quinoline, triazole, chalcone, EGFR, $BRAF^{V600E}$, Apoptosis, Docking.

Graphical Abstract

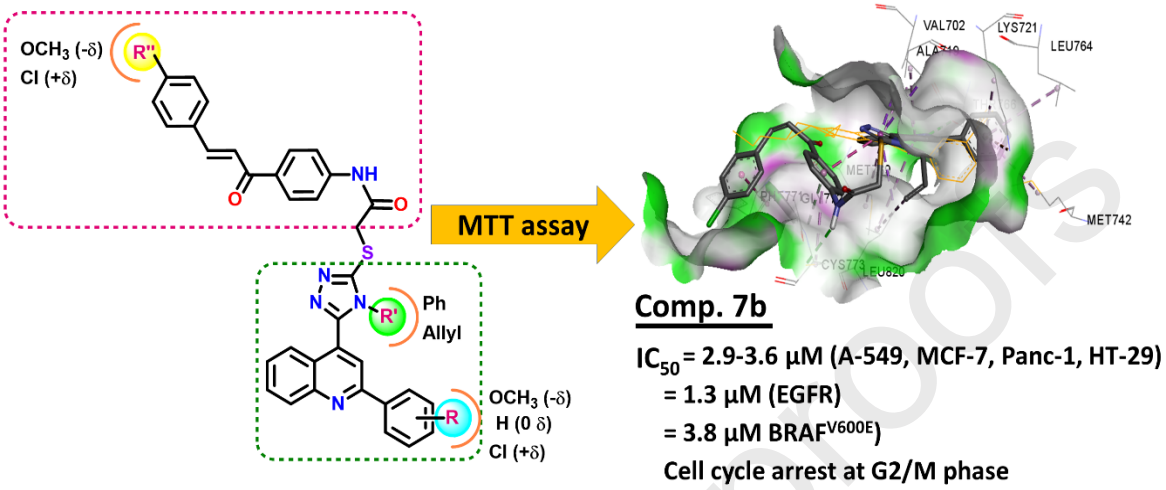

Comp. 7b

IC_{50} = 2.9-3.6 µM (A-549, MCF-7, Panc-1, HT-29)
= 1.3 µM (EGFR)
= 3.8 µM $BRAF^{V600E}$)
Cell cycle arrest at G2/M phase

Highlights

- A series of quinoline/chalcone hybrids containing 1,2,4-triazole moiety was synthesized and tested by NCI for their anticancer activity.
- Compounds **7b**, **7d**, **9b**, and **9d** were the most active ones with a growth inhibition percent between 77 and 94%.
- *In vitro* antiproliferative activity was evaluated using MTT assay.
- **7a, 7b, 9a, 9b,** and **9d** showed promising antiproliferative activities and were evaluated against EGFR and $BRAF^{V600E}$.
- A docking study of compounds **7a, 7b, 9a, 9b, and 9d** showed good binding affinities towards EGFR and $BRAF^{V600E}$.

1. INTRODUCTION

Cancer is a major global public health concern [1]. In developed countries, it presents a huge burden on society and economy. The incidence of cancer increases as population growth and aging increase, as well as the prevalence of other established risk factors [2]. It is estimated that there will be a 3-fold increase in the incidence of cancer in Egypt by 2050 compared to 2013 statistics [3]. Medicinal chemists are therefore faced with a challenging task of developing new anti-cancer agents to overcome the spread of cancer, either in Egypt or around the world [4].

Quinoline derivatives are common, broad-spectrum drugs [5]. Quinoline moiety can be recognized in many bioactive compounds including anti-cancer [6], anti-inflammatory [7, 8], antiviral [9], antimicrobial [10], and anti-parasitic agents [11]. Recently, several research papers have described quinoline derivatives with anti-cancer activity, which can be observed by an increasing number of published reviews of the chemistry and biological activity of anti-cancer quinolines [6, 12, 13]. Quinoline derivatives act as anti-cancer agents through a variety of mechanisms, including inhibition of cell growth, promoting factors such as tubulin polymerization, topoisomerase, tyrosine kinase, proteasome, tyrosine kinase, and DNA repair [4,14].

Recently, due to their effective therapeutic importance, attention has been paid to the chemistry of triazoles and their derivatives [15]. The 1,2,4-triazole ring could be considered as an ester, amide, carboxylic acid, and other heterocycle isostere [16]. The 1,2,4-triazole-containing ring system is a common pharmacophore that has been incorporated into a wide range of therapeutically interesting active compounds. For example, anti-cancer [17], anti-inflammatory [18], anti-microbial [19], analgesic [20], anti-viral, [21] and anti-convulsant [22] active compounds.

Chalcones are an important category of flavonoid family derived from synthetic or natural compounds [23]. Due to their versatile therapeutic activities, such as anti-cancer [24, 25], the production of chalcones as privileged scaffolds in medicinal chemistry has attracted great interest. Chalcones are proposed to cause cell-cycle disruption and apoptosis, inhibit tubulin polymerization, inhibit unique kinases that are essential for cancer cell proliferation and survival [26].

Over the last three decades, many hybrid molecules have been of great importance in the development of new drugs and have undergone clinical trials for the treatment of various diseases [27, 28]. Hybridization strategy has been used to develop new anti-cancer drugs by fusing more than two or more active pharmacophores in a single hybrid molecule with synergistic anti-cancer activity [29]. Hybrid molecules are designed to enhance the biological spectrum and efficacy, overcome drug cross resistance, and reduce potential toxicity compared to the parent drugs. For example, Hybridization of quinoline ring with 1,2,4-triazole ring in compounds **I** and **II (Fig. 1)** were found to induce apoptosis and inhibit cellular growth and proliferation of SB-590885-sensitive and SB-590885-resistant 451Lu melanoma cell lines, harboring $BRAF^{V600E}$ mutation, *via* inhibition of STAT3 phosphorylation with IC_{50} values ranging from 4.7 μM to 17 μM [30].

Hybridization of 1,2,4-triazole ring with chalcone moiety in compound **III** exhibited significant growth inhibition and induced caspase-3 dependent apoptosis in A549 human lung adenocarcinoma cells with IC_{50} value of 4.4 μM relative to cisplatin with IC_{50} value of 15.3 μM [25] (**Fig. 1**).

On the other hand, a growing number of research studies have been focused on the optimization and incorporation of quinoline and chalcone scaffolds into chemotherapeutic agents as it has been reported that combining quinoline and chalcone moieties in one compact structure leads to more potent cytotoxic activity [31, 32]. For instance, compound **IV**, a quinoline-chalcone hybrid, was reported to have a remarkable cytotoxic activity against different cancer cell lines. Compound **IV** could induce G2/M cell cycle arrest and apoptosis in A549 cancer cells (**Fig. 1**) [4].

Following the previous study on the importance of hybrid molecules in the treatment of different types of cancer and pathways, Herein, we report the design and synthesis of certain novel quinoline / chalcone derivatives (**7a-f**, **8a-f**, and **9a-f**, **Fig. 1**) that incorporate quinoline, chalcone and triazole rings into a single compact structure for synergistic anti-cancer activity, manage drug resistance development, and reduce possible side effects. Prepared compounds have different substitutions for the electron donating and the electron withdrawing groups for the SAR study of these compounds. The synthesized derivatives were evaluated for NCI cytotoxic assay and *in-vitro* antiproliferative activity against four different cancer cell lines: pancreas cancer cell line (Panc-1), breast cancer cell line (MCF-7), colon cancer cell line (HT-29), and epithelial cancer cell line (A-549). Furthermore, the most potent compounds were evaluated for their ability to inhibit EGFR and $BRAF^{V600E}$ as a potential mechanism for these compounds. The most potent derivatives were docked into the ATP binding sites of EGFR and $BRAF^{V600E}$.

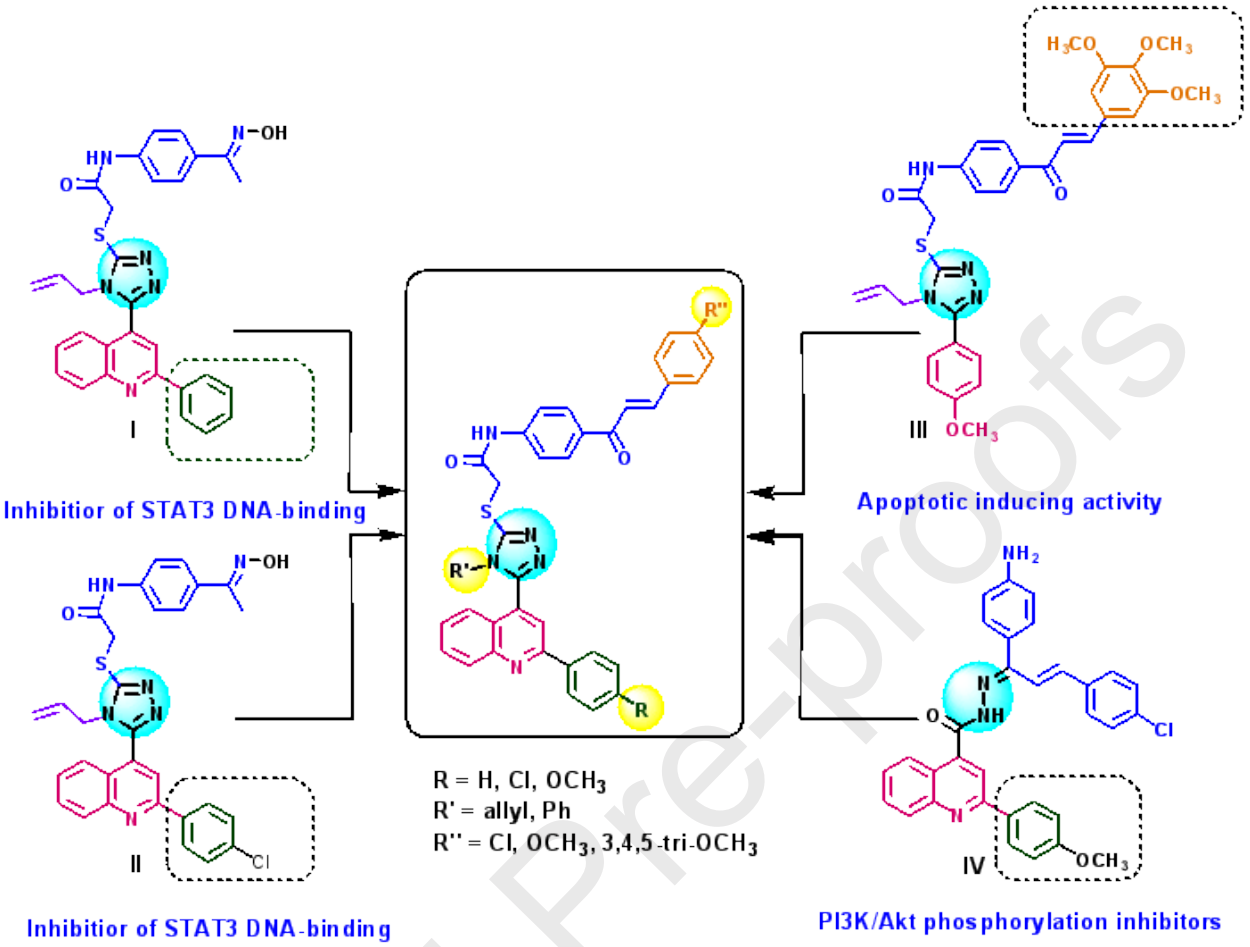

Fig. 1. Structures of representative hybrids **I-IV** and newly hybrids **7a-f**, **8a-f**, and **9a-f**

2. RESULTS AND DISCUSSION

2.1. Chemistry

The sequence of reactions used to synthesize quinoline-chalcone hybrids **7a-f**, **8a-f** and **9a-f** is obtained in **Scheme 1**. Synthesis of 2-(substituted phenyl) quinoline-4-carboxylic acids **1a–c** was performed by refluxing isatin with an appropriate acetophenone in aqueous ethanol [33]. Separate acids were refluxed with absolute ethanol in the presence of conc. H_2SO_4 as a dehydrating agent providing the corresponding esters **2a-e** [34]. Heating at reflux temperature of ethyl esters **2a-e** with hydrazine monohydrate afforded carbohydrazide derivatives **3a-c** [35]. The appropriate carbohydrazide **3a-e** was heated at reflux temperature with allyl or phenyl isothiocyanate in

ethanol, then aqueous 2N NaOH was added followed by acidification with conc. HCl affording 1,2,4-triazole-3-thiol derivatives **4a-f** [36]. Structures of the formed compounds have been confirmed by their reported melting points, ^{1}H NMR and ^{13}C NMR spectra. The acetylated chalcone intermediates **6a-c** were prepared according to the reported procedure [37] by reaction of the appropriate chalcone **5a-c** with bromoacetyl bromide using potassium carbonate as a base in dichloromethane. The separated compounds were coupled with 1,2,4-triazole-3-thiol derivatives **4a-f** in presence of acetonitrile and triethylamine (TEA) as base affording target compounds **7a-f**, **8a-f**, and **9a-f**. The structure of these novel compounds has been validated by NMR spectroscopy and mass spectral analysis.

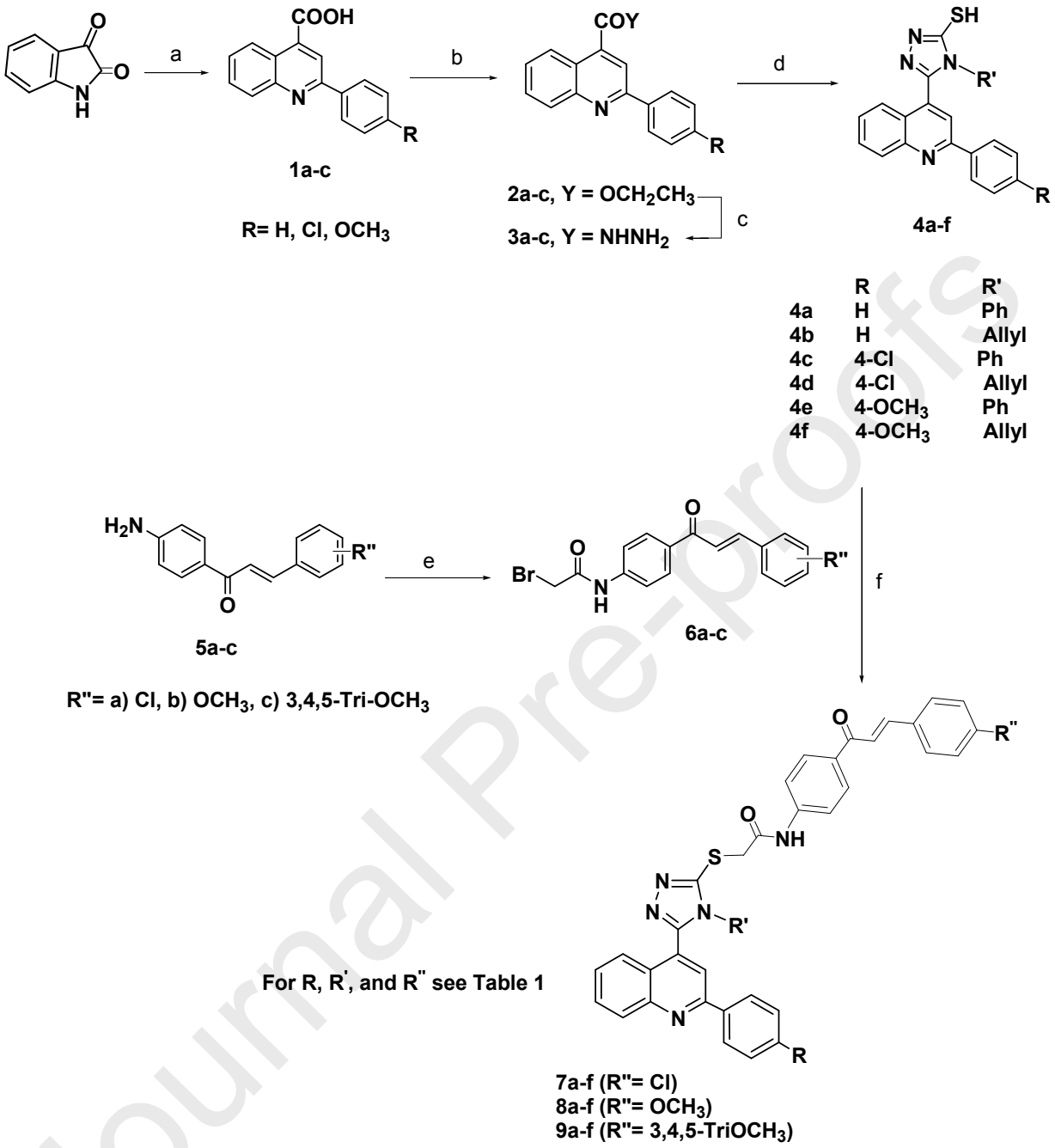

Scheme1: Synthesis of quinoline-chalcone hybrids **7a-f**, **8a-f**, and **9a-f**

Reagent and reaction conditions: (a) Appropriate acetophenone, EtOH, Reflux, 9–18 h; (b) EtOH, Conc. H_2SO_4, reflux 10 h; (c) NH_2NH_2, EtOH, reflux 3-7 h; (d) Appropriate isocyanate, EtOH, reflux, 5 h; (e) Bromoacetyl bromide, K_2CO_3, rt, 18 h; (f) TEA, Acetonitrile, rt, 4-8 h.

The ^{1}H NMR spectrum of **8f** as a representative example showed the appearance of the amidic NH signal and four sets of doublets at 8.04 and 7.82, and 7.08 and 6.96 ppm, which is indicative of aromatic *p*-disubstitution, 3 signals attributed to the allyl protons in the form of multiplet (1H) at 5.83-5.77 ppm, two sets of doublets at 5.32 and 5.05 (2H), and doublet signal (2H) at 4.49 ppm. In addition to singlet signal of two protons corresponding to SCH_2 and two signals with three proton integrations each at 3.92 (s) and 3.88 (s) ppm attributed to two methoxy. The ^{13}C NMR spectrum of **8f** showed the appearance of two carbonyl carbon signals at δ 188.99 (CH=CHCO), 166.77 (NHCO), a resonance at 36.99 ppm which was assigned to methylene carbon of SCH_2, and two resonances at 142.30 and 124.60 ppm which were assigned to CH=CH as well as the allyl carbons. The structure was also confirmed by HRESI-MS with $[M+H]^+$ ion at m/z 668.2379 which correlates with the molecular weight and molecular formula $C_{39}H_{34}N_5O_4S$ of **8f**.

2.2. Evaluation of biological Activities

2.2.1. Screening of cytotoxic activity by NCI

A total of eighteen compounds were selected by the National Cancer Institute (NCI) for anticancer screening according to the protocol of the Drug Evaluation Branch of the National Cancer Institute, Bethesda, USA [38]. *In-vitro* anticancer screening was carried out in 60 cell lines of nine different cancer cell types: leukemia, ovarian, renal, prostate, melanoma, lung, CNS, colon, and breast cancers. Compound **7b** exhibited the most promising anti-cancer activity among all the tested compounds. It showed remarkable inhibitory activity against leukemia (K-562, MOLT-4, and SR), colon (HCT-15 and SW-620), ovarian (OVCAR-8), and breast (MCF7) cancer cell lines with percent growth inhibition in the range of 72.37-94.60% **(supplementary data)**. In addition, compound **7b** lead to complete cell death against colon (HCT-116), melanoma (LOX IMVI), and ovarian (IGROV1) cancer cell line. Compound **9b** had percent growth inhibition of 78.72% and 79.57% against breast (MCF7) and colon (HCT-116), respectively **(supplementary data)**. Compound **7d** exhibited moderate growth inhibition (66%) specifically against colon (HCT-116) cell line although it had a weak overall mean growth. Compound **9d** had an overall weak mean growth percent inhibition of 82% against all cancer cell lines, but he specifically caused complete cell death against leukemia (RPMI-8226) cell line and exhibited moderate growth inhibition ~ 56% against leukemia (MOLT-4), breast (MCF7), renal (UO-31 and RXF 393), ovarian (OVCAR-8), and colon (HCT-116 and HCT-15) cancer cell lines. Also, compounds **8d**, **9c**, and **9f** with weak overall mean growth percent inhibition of 90%, 94.30%, and 90.05%, respectively **(supplementary data)**. Nevertheless, compounds **8d** and **9c** had moderate growth inhibition of 55% and 41%, respectively against renal (UO-31) cell line. While compound **9f** experienced moderate growth inhibition of 45% and 50% against leukemia (RPMI-8226 and SR) cell lines,

respectively **(supplementary data)**. From the abovementioned results it could be generally detected that quinoline-chalcone derivatives with **R"** = 4-Cl or 3,4,5-TriOCH_3 substituents introduced more potent growth inhibitory activity against most of cancer cell lines on the contrary with other derivatives with R"= 4-OCH_3 that exhibited weak activity.

2.2.2 Cell viability assay

Cell viability testing using human mammary epithelial cell line (MCF-10A) was performed. with MCF-10A cells were treated with compounds **7a-f**, **8a-f**, and **9a-f** for 4 days and cell viability was assessed using a 3-(4,5-dimethylthiazole-2-yl)-2,5-diphenyltetrazol (MTT) test. All compounds were found to be non-toxic, most of which had a cell viability of over 82% at a concentration of 50 μM.

2.2.3. Antiproliferative effects

Propidium iodide (PI) tests were used to evaluate the antiproliferative activities of all selected compounds in four cancer cell lines, pancreatic cancer cell line (Panc-1), breast cancer cell line (MCF-7), cell line colon cancer (HT-29) and epithelial line cancer cell (A-549) and doxorubicin was used as the reference compound. GraphPad Prism software (GraphPad Software, San Diego, CA, USA) was used to calculate the median inhibition concentration (IC_{50}) for all compounds. Based on IC_{50}, an interesting relationship between analogs and their structural characteristics was observed.

As illustrated in **Table 1**, five most active compounds **7a, 7b, 9a, 9b,** and **9d** among both (4-phenyl-5-(2-phenyl-quinolin-4-yl)-1,2,4-triazol-3-ylsulfanyl-acetamide (R' = Ph and R" = Cl) and (4-allyl-5-(2-phenyl-quinolin-4-yl)-1,2,4-triazol-3-ylsulfanyl-acetamide (R' = Allyl and R" =3,4,5-TriOCH_3) derivatives exhibited potent inhibition of cancer cells growth. After compound **7b**,

almost comparable and extreme anti-cancer activity was observed between **9b** and **9d** compounds with both GI_{50} cell lines of 3.625 μM and 4.750 μM, respectively. While compound **7b** showed the highest activity among all new compounds against cancer cell growth with GI_{50} 3.325 μM. When comparing the effects on different cell lines of the individual compound, the findings of these most active compounds were almost similar with a slight difference in GI_{50} values from all four-cancer cell lines. All other compounds had weak to moderate effects on cancer cell growth.

Compound **7b (R = H**, **R' = Allyl** and **R'' = Cl)** displayed the highest anticancer potential and it was bearing allyl-triazole backbone while on the other side compound **7a (R = H**, **R' = Ph** and **R'' = Cl)** was bearing same substitution pattern as compared to **7b** and difference was phenyl-triazole moiety but it showed almost 2.5 folds less activity. Obviously, it can be concluded that all seven compounds belonging to allyl-triazole backbone **(7b**, **7d**, **8b**, **8d**, **8f**, **9b**, and **9f)** were better inhibitors of cancer cell growth as compared to other derivatives **(7a**, **7c**, **8c**, **8e**, **9a**, **9c**, and **9e)** bearing same substitutions but different backbone of phenyl-triazole.

Presence of different functional groups on terminal 3-phenyl acryloyl moiety (R'') exhibited a remarkable change in activity as compared to various groups on phenyl moiety in the quinoline ring (**R**). The presence of the 3,4,5-trimethoxy group on the 3-phenyl acryloyl ring showed a significant difference from the other groups and was found to be responsible for maximum activity after chloro group at same position. It was analyzed that compound **7b** bearing chloro substitution at 3-phenyl acryloyl ring and unsubstituted (**R** = H) phenyl ring of quinoline moiety was discovered best antiproliferative agent and second most significant substitution was the presence of 3,4,5-trimethoxy group at phenyl ring of 3-phenyl acryloyl (**Compound 9b**) with best inhibitory property. Moreover, the mean GI_{50} values of derivatives **7e, 7f, 8e, 8f, 9e,** and **9f** were the lowest among the tested compounds, suggesting the importance of the *para* substitution in the

phenyl tail of quinoline moiety for the antiproliferative activity and correlating with higher antiproliferative effects and the activity increased with (R) in the order of H > Cl > OCH_3. Five most potent compounds (**7a**, **7b, 9a, 9b,** and **9d**) among the above-mentioned series were selected for anticancer mechanistic experiments including their effect on $BRAF^{V600E}$ and EGFR-TK.

Table 1. Antiproliferative activities of compounds **7a-f**, **8a-f**, and **9a-f**

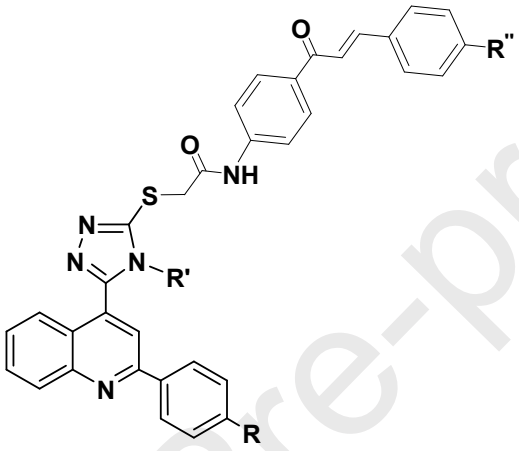

7a-f, **8a-f**, and **9a-f**

Compd.	R	R'	R"	Cell viability %	Anti-proliferative activity IC_{50}± SEM (μM)				
					A-549	**MCF-7**	**Panc-1**	**HT-29**	**Average**
7a	H	Ph	Cl	82	6.1±0.8	7.5±1.2	8.2±1.2	7.8±1.4	7.400
7b	H	Allyl	Cl	91	3.6±0.05	3.3±0.08	2.9±0.02	3.5±0.02	3.325
7c	4-Cl	Ph	Cl	79	31.6±3.8	35.4±2.7	36.0±1.9	34.7±3.2	34.425
7d	4-Cl	Allyl	Cl	89	15.2±0.6	14.9±0.3	15.8±1.5	14.9±0.8	15.200
7e	4-OCH_3	Ph	Cl	85	26.8±3.2	26.5±2.7	31.7±3.1	28.2±3.4	28.300
7f	4-OCH_3	Allyl	Cl	82	29.4±3.6	28.5±2.8	32.6±3.5	29.2±2.2	29.925
8a	H	Ph	OCH_3	87	20.4±3.2	19.5±2.7	21.7±3.1	21.2±3.4	20.700
8b	H	Allyl	OCH_3	84	23.5±0.2	23.1±0.1	23.3±0.2	23.9±0.6	23.450
8c	4-Cl	Ph	OCH_3	86	30.1±3.6	29.5±2.8	32.6±3.5	29.8±2.2	30.500
8d	4-Cl	Allyl	OCH_3	96	11.3±2.5	12.9±1.8	12.5±2.3	12.2±1.4	12.225
8e	4-OCH_3	Ph	OCH_3	89	25.5±2.6	25.6±2.2	25.6±2.9	25.8±1.4	25.375
8f	4-OCH_3	Allyl	OCH_3	91	24.5±2.6	23.6±2.2	24.6±2.9	24.8±1.4	24.375

9a	H	Ph	Tri-MeO	90	6.9±0.3	6.8±1.6	6.6±1.5	6.9±1.1	6.800
9b	H	Allyl	Tri-MeO	89	3.9±0.6	3.2±0.08	3.6±1.2	3.8±0.2	3.625
9c	4-Cl	Ph	Tri-MeO	84	16.4±1.3	15.4±5.2	18.6±2.5	16.9±3.7	16.825
9d	4-Cl	Allyl	Tri-MeO	92	4.7±0.4	4.9±0.6	4.5±0.2	4.9±0.2	4.750
9e	4-OCH_3	Ph	Tri-MeO	90	17.7±2.5	15.6±2.9	17.8±1.9	17.8±1.6	17.225
9f	4-OCH_3	Allyl	Tri-MeO	89	9.9±0.7	9.4±1.0	10.6±0.5	10.4±1.6	10.075
Doxorubicin		**--**	--	--	1.21 ± 0.80	0.90± 0.62	1.41 ± 0.58	1.01 ± 0.82	1.136

2.2.4. EGFR inhibitory activity assay

An assessment of the EGFR inhibitory ability of the most potent five derivatives was performed, and findings are included in **Table 2**. The results from this study support the findings of both cytotoxic activity by NCI and cancer cell-based assays. All investigated compounds **7a**, **7b, 9a, 9b,** and **9d** exhibited inhibition of EGFR with IC_{50} ranging from **1.3** to **4.8** μM. According to data presented, three derivatives (**9d**, **7b**, and **9b**) selected from allyl-triazole backbone were found to be most potent in comparison to the positive control erlotinib (IC_{50} = 0.08±0.04 μM). This study demonstrates that these compounds are effective EGFR inhibitors and may be used for future development as lead compounds.

2.2.5. $BRAF^{V600E}$ inhibitory activity

The $BRAF^{V600E}$ inhibitory ability of five most active synthesized compounds **7a**, **7b, 9a, 9b,** and **9d** were evaluated *in vitro*. All compounds analyzed showed IC_{50} within the range of **1.1 to 6.9** μM according to data in **Table 2**. It is noteworthy that two of allyl-triazole backbone (**9d** and **9b**) with the presence of R" = 3,4,5-tri-methoxy have the highest inhibitory potential for $BRAF^{V600E}$ and were also effective against the growth of cancer cells. The results of this assay show that the compounds examined are possible anticancer agents and effectively inhibit the BRAF enzyme.

Table 2. Effects of compounds **7a**, **7b**, **9a**, **9b** and **9d** on EGFR and $BRAF^{V600E}$

Compd	R	R'	R''	EGFR inhibition $IC_{50} \pm SEM$ (μM)	$BRAF^{V600E}$ inhibition $IC_{50} \pm SEM$ (μM)
7a	H	Ph	Cl	4.8±1.7	6.9±1.7
7b	H	Allyl	Cl	1.3±1.2	3.8±1.5
9a	H	Ph	Tri-MeO	3.7±1.5	5.7±1.6
9b	H	Allyl	Tri-MeO	2.1±0.4	1.6±1.4
9d	4-Cl	Allyl	Tri-MeO	2.8±0.8	1.1±0.6
Erlotinib	--	--	--	0.08±0.04	0.06±0.04

2.2.6. Cell cycle analysis and apoptosis detection

2.2.6.1. Cell cycle analysis

Studies have been conducted on the effect of compound **7b** on growth and apoptosis in the Panc-1 cell cycle. Panc-1 cells were incubated with an IC_{50} concentration (2.9 μM) of **7b** for 24 h. The results of the study (**Fig. 2**) reveal that the pre-G1 apoptosis rate of compound **7b** on Panc-1 was 27.15%. In G2/M phase, a high percent of cell accumulation was observed in Panc-1 treated with **7b** (34.36%) indicating cell cycle arrest at G2/M transition.

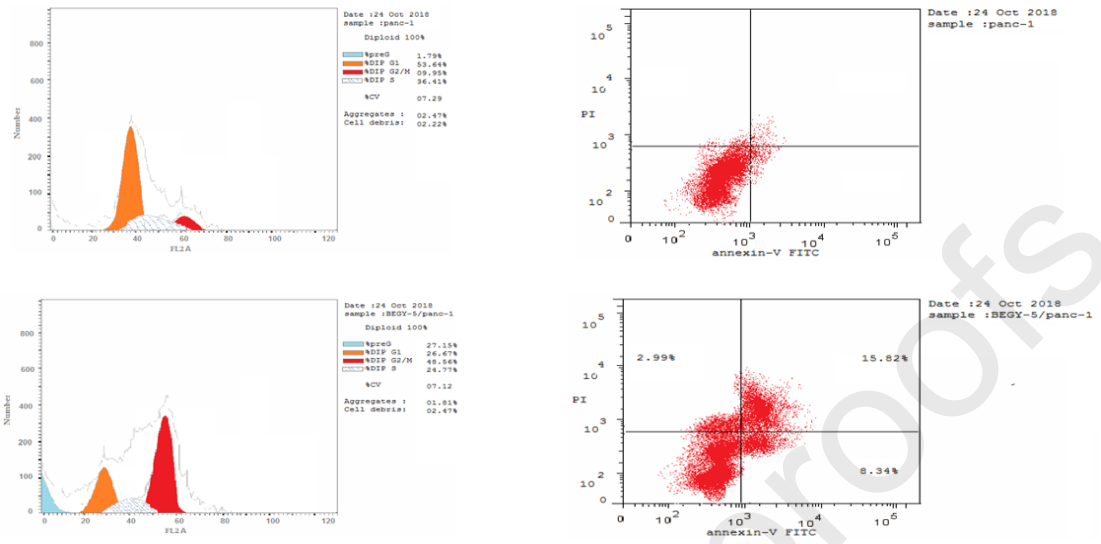

Fig. 2. Cell cycle analysis in Panc-1 cell line treated with compound **7b**

2.2.6.2. Apoptosis assay

Analysis of the Panc-1 cell cycle showed that pre-G1 apoptosis signalling occurred after **7b** treatment. Annex V/ PI was labelled in cells and incubated 24 hours to check **7b** for apoptosis cells. Early and late apoptosis studies have shown that **7b** with 2.99% necrosis is likely to cause significant apoptosis, **(Table. 3)**.

Table 3. Apoptosis detection of **7b** in Panc-1 cancer cell line.

Compound	**Apoptosis**			**Necrosis**
	Total	**Early**	**Late**	
7b/panc-1	27.15	8.34	15.82	2.99
Control/panc-1	1.79	1.02	0.47	0.3

2.3. Docking study into EGFR and BRAF^{V600E}

In the current study, the biological evaluation of the new compounds (**7a**, **7b, 9a, 9b,** and **9d**) revealed inhibitory activity against EGFR and BRAF^{V600E} kinases, **Table 2**. Accordingly, we have performed a molecular docking study to evaluate the binding modes, orientations and interactions of these compounds into the ATP binding sites of EGFR (pdb code: 1M17) (38) and BRAF^{V600E} (pdb code: 3OG7) (39). The crystal structures of the two kinases were obtained from the Protein Data Bank (https://www.rcsb.org/structure).

AutoDock 4.2 (40) was used in the docking study. Ligand and protein files were prepared according to the previous reports (41, 42). Grid and docking parameter files were prepared by AutoDock tools (ADT) following the previous reports (43, 44). Visualization of the 2/3D binding modes of the new compounds was performed by Discovery Studio Visualizer (45). To validate the docking procedures, the co-crystallized ligands, erlotinib and vemurafenib were initially re-docked into the active site of EGFR and BRAF^{V600E}, respectively. The results revealed superposition of erlotinib and vemurafenib over the native ligands, **Fig. 3**. Moreover, the re-docked ligands exhibited similar binding interactions to those of the corresponding co-crystallized ligands

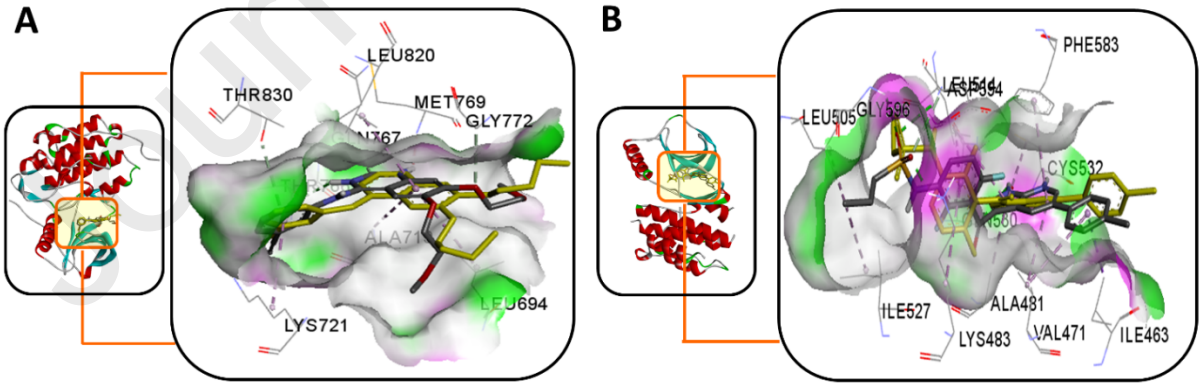

Fig. 3. Binding mode/interactions of redocked/co-crystallized erlotinib and vemurafenib into their corresponding kinases: A) binding mode of the redocked erlotinib (shown as sticks, colored by element) into the ATP binding site of EGFR (PDB code: 1M17) overlaid with the co-crystallized

ligand (show as line, colored in blue) with RMSD of 1.44 Å; B) binding mode of redocked vemurafenib (shown as sticks, colored by element) into the ATP binding site of BRAFV600E (pdb code: 3OG7) overlaid with the co-crystallized ligand (show as line, colored in blue) with RMSD of 1.44 Å. Receptor shown as hydrogen bond surface.

The molecular docking analyses revealed that the new compounds adopted binding conformations into the active site of EGFR in which the chalcone-bearing side chain are folded toward the triazole ring inside the front hydrophobic pocket of the two kinases. this conformation allows the new compounds to occupy small volume and fit into the active site of EGFR without any steric clashes or unfavorable interactions. Moreover, the new compounds exhibited higher binding affinities (ΔG_b = -9.94 to -11.43 kcal/mol) for the five compounds (**7a**, **7b, 9a, 9b,** and **9d**) compared to erlotinib (ΔG_b = -7.39 kcal/mol), **Table 4**. However, the tested compounds exhibited weaker inhibitory activity against EGFR compared to erlotinib. Accordingly, other parameters such as binding interactions and conformations of the new compounds were investigated to understand their inhibitory activities. Among the docked derivatives, compound **7b** exhibited the highest binding free energy (ΔG_b = -11.43 kcal/mol) toward EGFR compared to -7.39 kcal/mol for erlotinib, **Table 4**. These results were matched with the *in vitro* inhibitory activity of the new compounds against EGFR, **Table 2**.

Investigation of the binding orientation of compound **7b** revealed that it adopted an orientation in which the 2-phenyl group occupy the hydrophobic pocket like the cyanophenyl group of erlotinib. The quinoline ring of compound **7b** overlaid partially over the quinazoline ring in erlotinib. The 4-(3-(4-chlorophenyl)acryloyl)phenyl moiety in compound **7b** is folded toward the triazole ring which decreases the molecular volume of the compound and allowed it to occupy the front hydrophobic pocket in EGFR, **Fig. 4**.

Table 4. Results of the docking of compounds **7b** and **9d** into EGFR (pdb: 1M17) [54] and $BRAF^{V600E}$ (pdb code: 3OG7) [55] in comparison to its co-crystallized ligand.

Kinase (pdb)	Ligand	ΔG_b [a]	K_i [b]	HBs [c]	Atoms in H-bonding		Length [d] (Å)
EGFR (1M17)	**7b**	-11.43	4.19 nM	3	Pyridine N	OH of Thr766	3.01
					Ph-NH [f]	NH of Cys773	2.98
					C=O	NH of Met769	2.12
					CONH	SH of Cys751	2.61
					CONH	C=O of Thr766	2.45
	9d	-9.94	51.45 nM	7	CONH	C=O of Gln767	2.89
					3/5-OCH_3 [e]	Gly695, Asp776, Thr830, Asp831	1.72-2.86
	AQ4	-7.39	3.84 µM	2	Met769	Met769	1.64
					CH-2 [e]	Gln767 [e]	2.06
$BRAF^{V600E}$ (3OG7)	**7b**	-9.84	61.08 nM	3	C=O	NH_2 of Lys483	2.45
					NH	C=O of Gln530	2.89
					C=O	NH of Asp594	2.49
	9d	-9.94	51.6 nM	5	4-OCH_3	NH_2 of Lys483	2.20
					C=O	NH of Cys532	1.83
					S	NH of Ser536	2..87
					3-OCH_3 [e]	Asn581	2.73
					3-OCH_3 [e]	Asp594	2.29
	032	-9.89	55.89 nM	3	Pyridine N	NH of Cys532	2.00
					SO_2	NH of Phe595	2.55
					SO_2	NH of Gly596	1.65

[a] Binding free energy (kcal/mol); [b] Inhibition constant; [c] number of hydrogen bond; [d] bond distance (angstrom); [e] carbon hydrogen bond; AQ4, erlotinib ([6,7-bis(2-methoxy-ethoxy)quinazoline-4-yl]-(3-ethynylphenyl)amine); 032, vemurafenib (N-(3-{[5-(4-chlorophenyl)-1H-pyrrolo[2,3-b]pyridin-3-yl]carbonyl}-2,4-difluorophenyl)propane-1-sulfonamide)

Investigation of the binding interactions of compound **7b** revealed two conventional hydrogen bonds with Thr766 and Cys773 compared to only one hydrogen bonds for erlotinib. Compound **7b** also exhibited one carbon hydrogen bond with CYS773 and one pi-sulfur interaction with Lys721. In addition, compound **7b** showed several types of hydrophobic interactions with hydrophobic residues such as Ala719, Met742, Met769, and Phe771 in EGFR, **Fig. 4**.

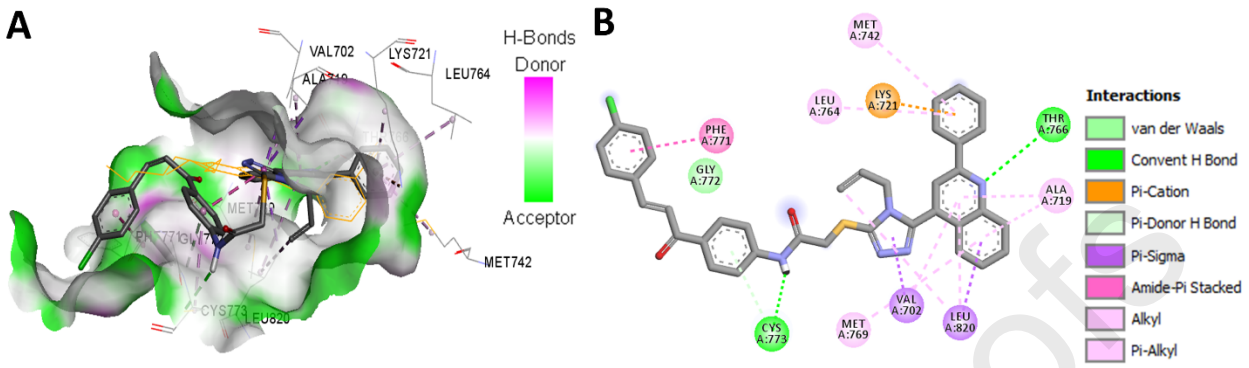

Fig. 4. Binding modes/interactions of compound **7b** into EGFR (PDB code: 1M17): A) 3D binding mode of compound **7b** into the active site of EGFR, the co-crystallized erlotinib shown as orang line, receptor shown as hydrogen bond surface, hydrogen atoms were omitted for clarity; B) 2D binding mode of compound **7b** into EGFR showing different types of interactions with amino acids in the active site, hydrogen atoms were omitted for clarity.

In addition, the docking results revealed that compounds **7a** and **9a** have lower binding affinities than compounds **7b** and **9b**. Moreover, compound **9a** showed slightly higher affinity toward EGFR than compound **7a**, **Table 4**. These results were matched with the *in vitro* inhibitory activity of the four compounds, **Table 2**. On the other hand, compounds **7a** and **9a** exhibited slightly binding affinities compared to that of compound **9d** although they were less active *in vitro*. These results could be attributed to the higher number of hydrogen bonds observed with compound **9d**. In addition.

The new compounds (**7a**, **7b, 9a, 9b,** and **9d**) were docked into $BRAF^{V600E}$ (pdb code: 3OG7) [55]. The results of the docking study revealed that the five high binding affinities (ΔG_b = -9.11 to -9.94 kcal/mol) which were comparable to that of vemurafenib (ΔG_b = -9.89 kcal/mol), **Table 4**.

Compound **9d** displayed the highest binding free energy (ΔG_b = of -9.94 kcal/mol) toward $BRAF^{V600E}$ compared to -9.89 kcal/mol for vemurafenib, **Table 4**. Compound **9d** displayed three conventional hydrogen bonds with Lys483, Cys532 and Ser536 with bond length in the range of

1.83-2.87 Å. In addition, compound 9d showed two carbon hydrogen bonds between with Asn581 Asp594 amino acids. One pi-sulfur interaction with Phe583 and several hydrophobic interactions with Ile463, Leu514, and Tyr538 were also observed for compound **9d**, **Fig. 5**. The high binding affinity and the interaction pattern of compound 9d could account for its high activity against $BRAF^{V600E}$, **Table 2**.

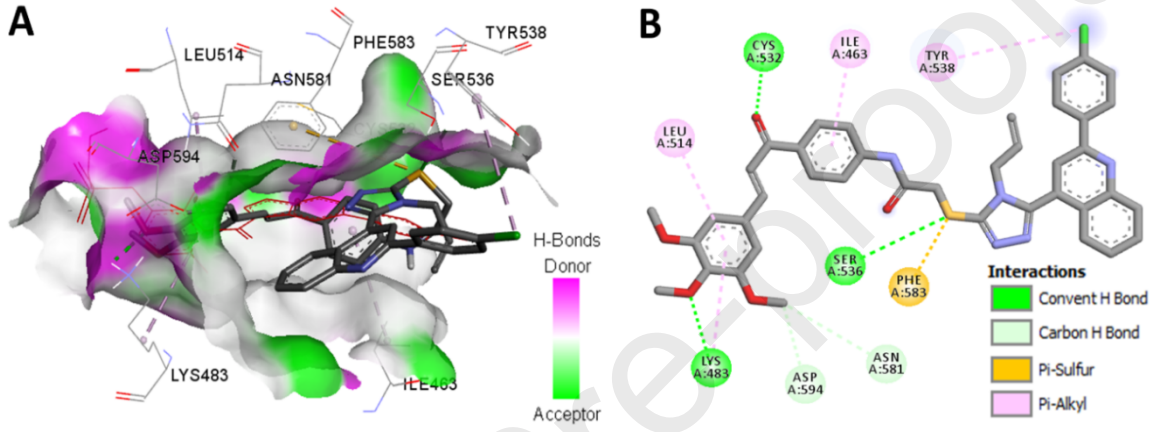

Figure 5: Binding modes/interactions of compound **9d** into $BRAF^{V600E}$ (pdb code: 3OG7)**:** A) 3D binding mode of compound **9d** into the active site of $BRAF^{V600E}$, vemurafenib shown as brown line, receptor shown as hydrogen bond surface, hydrogen atoms were omitted for clarity; B) 2D binding mode of compound **9d** into $BRAF^{V600E}$ showing different types of interactions with amino acids in the active site, hydrogen atoms were omitted for clarity.

The binding modes, orientations, and interactions of compound **7a, 9a, and 9b** into the active site of EGFR and $BRAF^{V600E}$ are provided in supplementary data (**Figs. S1-8**).

3. CONCLUSION

Eighteen novel quinoline / chalcone hybrids containing 1,2,4-triazole moiety have been designed, synthesised, and submitted to NCI for an anticancer activity assessment. The newly synthesized hybrids were tested *in vitro* against a panel of cancer cell lines and EGFR and $BRAF^{V600E}$ anticancer targets. Some of the compounds analysed had a significant inhibitory anti-proliferative effect. The most potent compounds were **7a**, **7b**, **9a**, **9b** and **9d**. Compounds **9d**, **7b**, and **9b** selected from allyl-triazole backbone were found to be most potent in comparison to the positive control erlotinib. The results of $BRAF^{V600E}$ inhibitory assay show that the compounds examined are possible anticancer agents and effectively inhibit the $BRAF^{V600E}$ enzyme. Compound **7b** induced apoptosis and demonstrated cell cycle arrest in G2/M phase. To understand the results of the kinases inhibitory activities of compounds **7a, 7b, 9a, 9b,** and **9d**, a molecular docking study was performed into the active sites of EGFR and $BRAF^{V600E}$. The results revealed nice fitting into the active sites of the two kinases. The new compounds also exhibited higher binding free energies toward EGFR than the native ligand, erlotinib. Moreover, these compounds displayed binding affinities toward $BRAF^{V600E}$ comparable to that of vemurafenib.

Acknowledgment

Not applicable

Conflicts of interest

The authors declare no conflict of interest

4. EXPERIMENTAL

4.1. Chemistry

General details: **See Appendix A**

4.1.1. General procedure for the synthesis of compounds (7a-f, 8a-f, and 9a-f).

An equimolar mixture of compounds **4a-f**, compounds **6a-c** and TEA (1.2 mmol) in acetonitrile (50 mL) was stirred at RT for 4-8 h. The resulting precipitate is filtered off, dried and then applied to Silica gel 60 N to obtain pure product using the DCM/EA (9:1) as eluent system to afford the pure novel products **7a-f**, **8a-f**, and **9a-f**.

4.1.1.1. 2-(4-Phenyl-5-(2-phenylquinolin-4-yl)-4*H*-1,2,4-triazol-3-ylthio)-*N*-(4-((*E*)-3-(4-chlorophenyl)acryloyl)phenyl)acetamide (7a).

Pale yellow solid (61%); m.p. 261-262 ^{o}C; IR (FT-IR, cm^{-1}): 3328 (NH), 1698 (C=O), 1659 (CO-NH); ^{1}H NMR (600 MHz, DMSO-d_6) δ (ppm): 10.85 (s, 1H, NH), 8.22 (d, J = 9.0 Hz, 2H, Ar-H), 8.14 (d, J= 8.4 Hz, 1H, Ar-H), 8.11 (d, J = 7.8 Hz, 2H, Ar-H), 8.07 (s, 1H, Ar-H), 8.03 (d, J = 9.0 Hz, 1H, Ar-H), 8.00 (d, J = 15.6 Hz, 1H, CH=CH), 7.95 (d, J = 8.4 Hz, 2H, Ar-H), 7.84–7.81 (m, 3H, Ar-H), 7.73 (d, J = 15.6 Hz, 1H, CH=CH), 7.64–7.62 (m, 1H, Ar-H), 7.55–7.53 (m, 3H, Ar-H), 7.53–7.50 (m, 4H, Ar-H), 7.47–7.43 (m, 3H, Ar-H), 4.40 (s, 2H, S-CH_2); ^{13}C NMR (151 MHz, DMSO-d_6) δ (ppm): 187.46, 166.18, 155.19, 152.06, 151.85, 147.82, 147.81, 143.26, 141.95, 137.77, 134.97, 133.76, 133.17, 133.12, 132.50, 130.50, 130.05, 129.98, 129.78, 129.53, 128.93, 128.91, 127.48, 127.32, 126.98, 125.53, 124.52, 122.76, 120.39, 118.56, 37.00; MS (FAB) m/z 678.3 $(M+H)^{+}$; HRMS (FAB). Calcd for $C_{40}H_{29}O_2N_5ClS$: 678.1730. Found: 678.1729.

4.1.1.2. 2-(4-Allyl-5-(2-phenylquinolin-4-yl)-4*H*-1,2,4-triazol-3-ylthio)-*N*-(4-((*E*)-3-(4-chlorophenyl)acryloyl)phenyl)acetamide (7b).

Yellow solid (79%); m.p. 237-238 ^{o}C; IR (FT-IR, cm^{-1}): 2969 (NH), 1690 (C=O), 1660 (CO-NH); ^{1}H NMR (600 MHz, DMSO-d_6) δ (ppm): 10.82 (s, 1H, NH), 8.31 (d, J = 7.2 Hz, 1H, Ar-H), 8.30 (s, 1H, Ar-H), 8.21–8.19 (m, 3H, Ar-H), 7.99 (d, J = 15.6 Hz, 1H, CH=CH), 7.94 (d, J = 8.4 Hz, 2H, Ar-H), 7.89–7.85 (m, 2H, Ar-H), 7.82 (d, J = 9.0 Hz, 2H, Ar-H), 7.73 (d, J = 15.6 Hz, 1H, CH=CH), 7.64–7.62 (m, 1H, Ar-H), 7.59 (d, J = 7.8 Hz, 2H, Ar-H), 7.55–7.53 (m, 3H, Ar-H), 5.90–5.82 (m, 1H, CH_2-CH=CH_2), 5.13 (d, J = 10.8 Hz, 1H, CH=CH_2), 4.84 (d, J = 16.8 Hz, 1H, CH=CH_2), 4.64 (d, J = 4.8 Hz, 2H, CH_2-CH), 4.35 (s, 2H, S-CH_2); ^{13}C NMR (151 MHz, DMSO-d_6) δ (ppm): 187.95, 166.84, 156.10, 152.51, 151.59, 148.49, 143.71, 142.45, 138.39, 135.45, 134.24, 134.13, 133.02, 132.98, 132.63, 131.09, 130.98, 130.53, 130.19, 129.43, 129.42, 128.08, 127.77, 125.65, 125.32, 123.25, 120.14, 119.07, 118.01, 47.21, 38.30; MS (FAB) m/z 642.1 $(M+H)^+$; HRMS (FAB). Calcd for $C_{37}H_{29}O_2N_5ClS$: 642.1730. Found: 642.1730.

4.1.1.3. 2-(5-(2-(4-Chlorophenyl)quinolin-4-yl)-4-phenyl-4*H*-1,2,4-triazol-3-ylthio)-*N*-(4-((*E*)-3-(4-chlorophenyl)acryloyl)phenyl)acetamide (7c).

Pale yellow solid (72%); m.p. 281-282 ^{o}C; IR (FT-IR, cm^{-1}): 3330 (NH), 1697 (C=O), 1660 (CO-NH); ^{1}H NMR (600 MHz, DMSO-d_6) δ (ppm): 10.84 (s, 1H, NH), 8.21 (d, J = 8.4 Hz, 2H, Ar-H), 8.12–8.08 (m, 5H, Ar-H), 7.99 (d, J = 15.6 Hz, 1H, CH=CH), 7.94 (d, J = 8.4 Hz, 2H, Ar-H), 7.84–7.81 (m, 3H, Ar-H), 7.73 (d, J = 15.6 Hz, 1H, CH=CH), 7.63 (t, J = 8.4 Hz, 1H, Ar-H), 7.60 (d, J = 8.4 Hz, 2H, Ar-H), 7.54 (d, J = 8.4 Hz, 2H, Ar-H), 7.52–7.50 (m, 2H, Ar-H), 7.46 – 7.42 (m, 3H, Ar-H), 4.40 (s, 2H, S-CH_2); ^{13}C NMR (151 MHz, DMSO-d_6) δ (ppm): 187.94, 166.65, 154.46, 152.57, 152.28, 148.21, 143.74, 142.44, 137.13, 137.03, 135.45, 134.25, 133.92, 133.54, 132.99, 131.13, 130.98, 130.53, 130.25, 130.01, 129.47, 129.42, 129.20, 128.19, 127.77, 126.00, 125.08,

123.25, 120.78, 119.05, 37.50; MS (FAB) *m/z* 712.0 $(M+H)^+$; HRMS (FAB). Calcd for $C_{40}H_{28}O_2N_5Cl_2S$: 712.1341. Found: 712.1335.

4.1.1.4. 2-(4-Allyl-5-(2-(4-chlorophenyl)quinolin-4-yl)-4*H*-1,2,4-triazol-3-ylthio)-*N*-(4-((*E*)-3-(4-chlorophenyl)acryloyl)phenyl)acetamide (7d).

Off-white solid (78%); m.p. 255-256 ^oC; IR (FT-IR, cm^{-1}): 3244 (NH), 1698 (C=O), 1658 (CO-NH); ^1H NMR (600 MHz, DMSO-d_6) δ (ppm): 10.82 (s, 1H, NH), 8.34 (d, *J* = 9.0 Hz, 2H, Ar-H), 8.32 (s, 1H, Ar-H), 8.22–8.19 (m, 3H, Ar-H), 7.99 (d, *J* = 15.6 Hz, 1H, CH=CH), 7.94 (d, *J* = 8.4 Hz, 2H, Ar-H), 7.90–7.84 (m, 2H, Ar-H), 7.82 (d, *J* = 9.0 Hz, 2H, Ar-H), 7.73 (d, *J* = 15.6 Hz, 1H, CH=CH), 7.66–7.63 (m, 3H, Ar-H), 7.54 (d, *J* = 8.4 Hz, 2H, Ar-H), 5.87–5.80 (m, 1H, CH_2-CH=CH_2), 5.11 (d, *J* = 10.5 Hz, 1H, CH=CH_2), 4.83 (d, *J* = 17.2 Hz, 1H, CH=CH_2), 4.64 (d, *J* = 4.2 Hz, 2H, CH_2-CH), 4.35 (s, 2H, S-CH_2); ^{13}C NMR (151 MHz, DMSO-d_6) δ (ppm): 187.46, 166.34, 154.42, 151.93, 151.13, 147.92, 143.22, 141.97, 136.71, 134.99, 134.13, 133.84, 133.76, 132.53, 132.10, 130.88, 130.73, 130.49, 130.04, 129.69, 128.98, 128.93, 128.27, 125.18, 124.92, 122.75, 119.59, 118.58, 117.57, 46.70, 37.79; MS (FAB) *m/z* 676.4 $(M+H)^+$; HRMS (FAB). Calcd for $C_{37}H_{28}O_2N_5Cl_2S$: 676.1341. Found: 676.1316.

4.1.1.5. 2-(5-(2-(4-Methoxyphenyl)quinolin-4-yl)-4-phenyl-4*H*-1,2,4-triazol-3-ylthio)-*N*-(4-((*E*)-3-(4-chlorophenyl)acryloyl)phenyl)acetamide (7e).

Pale yellow solid (68%); m.p. 281-282 ^oC; IR (FT-IR, cm^{-1}): 3310 (NH), 1697 (C=O), 1657 (CO-NH); ^1H NMR (600 MHz, DMSO-d_6) δ (ppm): 10.84 (s, 1H, NH), 8.21 (d, *J* = 8.4 Hz, 2H, Ar-H), 8.09 (d, *J* = 7.8 Hz, 1H, Ar-H), 8.05 (d, *J* = 8.4 Hz, 1H, Ar-H), 8.02 (d, *J* = 9.6 Hz, 3H, Ar-H), 7.99 (d, *J* = 15.6 Hz, 1H, CH=CH), 7.95 (d, *J* = 8.4 Hz, 2H, Ar-H), 7.83 (d, *J* = 9.0 Hz, 2H, Ar-H), 7.78 (t, *J* = 7.8 Hz, 1H, Ar-H), 7.73 (d, *J* = 15.6 Hz, 1H, CH=CH), 7.58 (t, *J* = 7.8 Hz, 1H, Ar-H), 7.55 (d, *J* = 8.4 Hz, 2H, Ar-H), 7.52 (d, *J* = 8.4 Hz, 2H, Ar-H), 7.47–7.42 (m, 3H, Ar-H), 7.07

(d, J = 9.0 Hz, 2H, Ar-H), 4.39 (s, 2H, S-CH_2), 3.84 (s, 3H, OCH_3); ^{13}C NMR (151 MHz, DMSO-d_6) δ (ppm): 187.95, 166.67, 161.41, 155.36, 155.34, 152.46, 152.42, 148.30, 143.74, 142.43, 135.45, 134.25, 133.61, 133.47, 132.99, 130.97, 130.85, 130.69, 130.53, 130.24, 129.78, 129.41, 128.95, 127.79, 127.47, 125.94, 124.68, 123.26, 120.49, 119.05, 114.81, 55.83, 37.51; MS (FAB) m/z 707.9 $(M+H)^+$; HRMS (FAB). Calcd for $C_{41}H_{31}O_3N_5ClS$: 708.1836. Found: 708.1846.

4.1.1.6. 2-(4-Allyl-5-(2-(4-methoxyphenyl)quinolin-4-yl)-4*H*-1,2,4-triazol-3-ylthio)-*N*-(4-((*E*)-3-(4-chlorophenyl)acryloyl)phenyl)acetamide (7f).

White solid (95%); m.p. 235-236 °C; IR (FT-IR, cm^{-1}): 3163 (NH), 1689 ($COCH_3$), 1660 (CONH); ^{1}H NMR (600 MHz, DMSO-d_6) δ (ppm): 10.82 (s, 1H, NH), 8.28 (d, J = 8.4 Hz, 2H, Ar-H)), 8.23 (s, 1H, Ar-H), 8.21 (d, J = 8.4 Hz, 2H, Ar-H), 8.15 (d, J = 8.4 Hz, 1H, Ar-H), 7.98 (d, J = 15.6 Hz, 1H, CH=CH), 7.94 (d, J = 8.4 Hz, 2H, Ar-H), 7.84–7.80 (m, 4H, Ar-H), 7.73 (d, J = 15.6 Hz, 1H, CH=CH), 7.58 (t, J = 8.4 Hz, 1H, Ar-H), 7.54 (d, J = 8.4 Hz, 2H, Ar-H), 7.13 (d, J = 8.4 Hz, 2H, Ar-H), 5.89–5.83 (m, 1H, CH_2-CH=CH_2), 5.13 (d, J = 10.2 Hz, 1H, CH=CH_2), 4.84 (d, J = 17.4 Hz, 1H, CH=CH_2), 4.63 (d, J = 4.2 Hz, 2H, CH_2-CH), 4.35 (s, 2H, S-CH_2), 3.87 (s, 3H, O-CH_3); ^{13}C NMR (151 MHz, DMSO-d_6) δ (ppm): 187.52, 166.35, 161.01, 157.94, 155.31, 152.13, 150.98, 148.03, 141.93, 134.96, 133.78, 133.50, 133.48, 132.12, 130.87, 130.46, 130.00, 129.47, 128.92, 128.77, 128.25, 127.08, 127.02, 125.08, 124.50, 119.26, 118.63, 117.57, 114.37, 55.36, 46.71, 37.88; MS (FAB) m/z 672.2 $(M+H)^+$; HRMS (FAB). Calcd for $C_{38}H_{31}O_3N_5ClS$: 672.1836. Found: 672.1854.

4.1.1.7. 2-(4-Phenyl-5-(2-phenylquinolin-4-yl)-4*H*-1,2,4-triazol-3-ylthio)-*N*-(4-((*E*)-3-(4-methoxyphenyl)acryloyl)phenyl)acetamide (8a).

White solid (89%); m.p. 275-276 °C; IR (FT-IR, cm^{-1}): 3176 (NH), 1693 (C=O), 1655 (CO-NH); ^{1}H NMR (600 MHz, DMSO-d_6) δ (ppm): 10.85 (s, 1H, NH), 8.19 (d, J = 8.4 Hz, 2H, Ar-H), 8.14

(d, *J* = 8.4 Hz, 1H, Ar-H), 8.11 (d, *J* = 8.4 Hz, 1H, Ar-H), 8.08 (s, 1H, Ar-H), 8.04 (d, *J* = 8.4 Hz, 2H, Ar-H), 7.86 (d, *J* = 8.4 Hz, 2H, Ar-H), 7.84–7.81 (m, 4H, Ar-H), 7.72 (d, *J* = 15.6 Hz, 1H, CH=CH), 7.62 (t, *J* = 7.8 Hz, 1H, Ar-H), 7.54–7.47 (m, 5H, Ar-H+CH=CH), 7.45–7.40 (m, 3H, Ar-H), 7.04 (d, *J* = 8.4 Hz, 2H, Ar-H), 4.39 (s, 2H, S-CH_2), 3.84 (s, 3H, OCH_3); ^{13}C NMR (151 MHz, DMSO-d_6) δ (ppm): 187.96, 166.62, 161.78, 155.69, 152.54, 152.33, 148.30, 143.92, 143.47, 138.26, 133.68, 133.61, 133.38, 131.86, 131.16, 130.99, 130.47, 130.30, 130.01, 129.40, 127.98, 127.90, 127.81, 127.47, 126.01, 125.01, 120.88, 119.98, 119.04, 114.90, 114.14, 55.87, 37.51; MS (FAB) *m*/*z* 673.9 $(M+H)^+$; HRMS (FAB). Calcd for $C_{41}H_{32}O_3N_5S$: 674.2226. Found: 674.2241.

4.1.1.8. 2-(4-Allyl-5-(2-phenylquinolin-4-yl)-4*H*-1,2,4-triazol-3-ylthio)-*N*-(4-((*E*)-3-(4-methoxyphenyl)acryloyl)phenyl)acetamide (8b).

White solid (90%); m.p. 205-207 °C; IR (FT-IR, cm^{-1}): 3161 (NH), 1689 (C=O), 1654 (CO-NH); ^{1}H NMR (600 MHz, DMSO-d_6) δ (ppm): 10.79 (s, 1H, NH), 8.31 (d, *J* = 8.4 Hz, 2H, Ar-H), 8.29 (s, 1H, Ar-H), 8.20 (d, *J* = 8.4 Hz, 1H, Ar-H), 8.18 (d, *J* = 9.0 Hz, 2H, Ar-H), 7.88 (d, *J* = 8.4 Hz, 2H, Ar-H), 7.85 (d, *J* = 9.0 Hz, 2H, Ar-H), 7.83–7.80 (m, 3H, Ar-H+CH=CH), 7.72 (d, *J* = 15.6 Hz, 1H, CH=CH), 7.63 (t, *J* = 7.8 Hz, 1H, Ar-H), 7.60–7.56 (m, 2H, Ar-H), 7.54 – 7.53 (m, 1H, Ar-H), 7.03 (d, *J* = 8.4 Hz, 2H, Ar-H), 5.89–5.83 (m, 1H, CH_2-CH=CH_2), 5.13 (d, *J* = 10.2 Hz, 1H, CH=CH_2), 4.84 (d, *J* = 17.4 Hz Hz, 1H, CH=CH_2), 4.65 (d, *J* = 4.8 Hz, 2H, CH_2-CH), 4.35 (s, 2H, S-CH_2), 3.84 (s, 3H, OCH_3); ^{13}C NMR (151 MHz, DMSO-d_6) δ (ppm): 187.96, 166.79, 161.78, 156.11, 152.51, 151.59, 148.49, 143.93, 143.42, 138.39, 134.14, 133.42, 132.62, 131.16, 131.10, 130.52, 130.31, 130.19, 129.44, 128.09, 127.89, 127.77, 125.65, 125.32, 120.14, 119.96, 119.06, 118.00, 114.90, 55.87, 47.21, 38.32; MS (FAB) *m*/*z* 638.2 $(M+H)^+$; HRMS (FAB). Calcd for $C_{38}H_{32}O_3N_5S$: 638.2226. Found: 638.2246.

4.1.1.9. 2-(5-(2-(4-Chlorophenyl)quinolin-4-yl)-4-phenyl-4*H*-1,2,4-triazol-3-ylthio)-*N*-(4-((*E*)-3-(4-methoxyphenyl)acryloyl)phenyl)acetamide (8c).

White solid (87%); m.p. 250-251 ^{o}C; IR (FT-IR, cm^{-1}): 3237 (NH), 1687 (C=O), 1654 (CO-NH); ^{1}H NMR (600 MHz, DMSO-d_6) δ (ppm): 10.82 (s, 1H, NH), 8.19 (d, J = 8.4 Hz, 2H, Ar-H), 8.12–8.08 (m, 5H, Ar-H+CH=CH), 7.86 (d, J = 8.4 Hz, 2H, Ar-H), 7.84–7.81 (m, 4H, Ar-H), 7.72 (d, J = 15.6 Hz, 1H, CH=CH), 7.61 (t, J = 8.4 Hz, 1H, Ar-H), 7.52 (d, J = 8.4 Hz, 2H, Ar-H), 7.51-7.50 (m, 2H, Ar-H), 7.45-7.42 (m, 3H, Ar-H), 7.04 (d, J = 8.4 Hz, 2H, Ar-H), 4.40 (s, 2H, S-CH_2), 3.84 (s, 3H, OCH_3);^{13}C NMR (151 MHz, DMSO-d_6) δ (ppm): 187.45, 166.12, 161.29, 153.97, 152.09, 151.79, 147.73, 143.43, 142.97, 136.55, 134.97, 133.43, 133.06, 132.89, 130.68, 130.64, 130.06, 129.83, 129.77, 129.52, 128.98, 128.71, 127.70, 127.41, 127.29, 125.52, 124.59, 120.30, 119.47, 118.54, 114.40, 55.37, 37.01; MS (FAB) m/z 708.5 $(M+H)^{+}$; HRMS (FAB). Calcd for $C_{41}H_{31}O_3N_5ClS$: 708.1836. Found: 708.1826.

4.1.1.10. 2-(4-Allyl-5-(2-(4-chlorophenyl)quinolin-4-yl)-4*H*-1,2,4-triazol-3-ylthio)-*N*-(4-((*E*)-3-(4-methoxyphenyl)acryloyl)phenyl)acetamide (8d).

White solid (57%); m.p. 230-232 ^{o}C; IR (FT-IR, cm^{-1}): 3176 (NH), 1687 ($COCH_3$), 1655 (CONH); ^{1}H NMR (600 MHz, DMSO-d_6) δ (ppm): 10.84 (s, 1H, NH), 8.39 (d, J = 9.0 Hz, 2H, Ar-H), 8.37 (s, 1H, Ar-H), 8.25–8.22 (m, 3H, Ar-H), 7.93–7.89 (m, 4H, Ar-H+CH=CH), 7.87-7.85 (m, 3H, Ar-H), 7.76 (d, J = 15.6 Hz, 1H, CH=CH), 7.71–7.68 (m, 3H, Ar-H), 7.08 (d, J = 8.4 Hz, 2H, Ar-H), 5.92–5.85 (m, 1H, CH_2-CH), 5.16 (d, J = 10.5, 1H, CH=CH_2), 4.88 (d, J = 17.4, 1H, CH=CH_2), 4.69 (d, J = 4.8 Hz, 2H, CH_2-CH), 4.40 (s, 2H, S-CH_2), 3.89 (s, 3H, OCH_3); ^{13}C NMR (151 MHz, DMSO-d_6) δ (ppm): 187.46, 166.29, 161.29, 154.41, 151.93, 151.13, 147.93, 143.44, 142.95, 136.71, 134.99, 133.84, 132.92, 132.11, 130.73, 130.67, 129.82, 129.69, 129.05, 128.97, 127.80,

127.41, 125.18, 124.92, 119.59, 119.47, 118.56, 117.56, 114.40, 55.37, 46.70, 37.81; MS (FAB) *m*/*z* 672.5 $(M+H)^+$; HRMS (FAB). Calcd for $C_{38}H_{31}O_3N_5ClS$: 672.1836. Found: 672.1836.

4.1.1.11. 2-(5-(2-(4-Methoxyphenyl)quinolin-4-yl)-4-phenyl-4*H*-1,2,4-triazol-3-ylthio)-*N*-(4-((*E*)-3-(4-methoxyphenyl)acryloyl)phenyl)acetamide (8e).

Pale yellow solid (65%); m.p. 295-296 °C; IR (KBr, cm^{-1}): 3413 (NH), 1600 (C=O), 1511 (CO-NH); ^1H NMR (600 MHz, DMSO-d_6) δ (ppm): 10.86 (s, 1H, NH), 8.22 (d, *J* = 8.7 Hz, 2H, Ar-H), 8.12 (d, *J* = 8.4 Hz, 1H, Ar-H), 8.08 (d, *J* = 8.4 Hz, 1H, Ar-H), 8.05 (d, *J* = 9.4 Hz, 3H, Ar-H), 7.89 (d, *J* = 8.7 Hz, 2H, Ar-H), 7.86–7.84 (m, 3H, Ar-H+CH=CH), 7.81 (t, *J* = 8.1 Hz, 1H, Ar-H), 7.75 (d, *J* = 15.6 Hz, 1H, CH=CH), 7.61 (t, *J* = 8.1 Hz, 1H, Ar-H), 7.57–7.53 (m, 2H, Ar-H), 7.48-7.47 (m, 3H, Ar-H), 7.09 (d, *J* = 8.8 Hz, 2H, Ar-H), 7.06 (d, *J* = 8.8 Hz, 2H, Ar-H), 4.43 (s, 2H, S-CH_2), 3.86 (s, 6H, 2 -OCH_3); ^{13}C NMR (151 MHz, DMSO-d_6) δ (ppm): 187.47, 166.14, 161.29, 160.92, 154.88, 152.00, 151.94, 147.82, 143.43, 142.97, 133.13, 132.99, 132.90, 130.67, 130.36, 130.21, 130.03, 129.83, 129.75, 129.29, 128.47, 127.41, 127.30, 126.98, 125.46, 124.19, 120.00, 119.48, 118.55, 114.40, 114.32, 55.32, 37.03; MS (FAB) *m*/*z* 704.6 $(M+H)^+$; HRMS (FAB). Calcd for $C_{42}H_{34}O_4N_5S$: 704.2332. Found: 704.2330.

4.1.1.12. 2-(4-Allyl-5-(2-(4-methoxyphenyl)quinolin-4-yl)-4*H*-1,2,4-triazol-3-ylthio)-*N*-(4-((*E*)-3-(4-methoxyphenyl)acryloyl)phenyl)acetamide (8f).

Yellow solid (62%); m.p. 124-125 °C; IR (FT-IR, cm^{-1}): 3260 (NH), 1691 (C=O), 1656 (CO-NH); ^1H NMR (600 MHz, $CDCl_3$) δ (ppm): 10.93 (s, 1H, NH), 8.27 (d, *J* = 8.4 Hz, 1H, Ar-H), 8.17 (d, *J* = 8.4 Hz, 2H, Ar-H), 8.04 (d, *J* = 9.0 Hz, 2H, Ar-H), 7.95 (s, 1H, Ar-H), 7.82 (d, *J* = 9.0 Hz, 2H. Ar-H), 7.81–7.79 (m, 3H, Ar-H+CH=CH), 7.63 (d, *J* = 8.4 Hz, 2H, Ar-H), 7.58 (t, *J* = 8.4 Hz, 1H, Ar-H), 7.44 (d, *J* = 15.6 Hz, 1H, CH=CH), 7.08 (d, *J* = 9.0 Hz, 2H, Ar-H), 6.96 (d, *J* = 9.0 Hz, 2H, Ar-H), 5.83–5.77 (m, 1H, -CH=CH_2), 5.32 (d, *J* = 10.2 Hz, 1H, CH=CH_2), 5.05 (d, *J*= 17.4 Hz,

1H, CH=$\underline{CH_2}$), 4.49 (d, *J* = 4.8 Hz, 2H, -$\underline{CH_2}$-CH), 4.14 (s, 2H, S-$\underline{CH_2}$), 3.92 (s, 3H, O$\underline{CH_3}$), 3.88 (s, 3H, O$\underline{CH_3}$); ^{13}C NMR (151 MHz, $CDCl_3$) δ (ppm): 188.99, 166.77, 161.62, 161.38, 156.17, 153.45, 148.87, 144.28, 142.30, 134.17, 132.50, 131.54, 131.00, 130.61, 130.31, 130.19, 130.12, 129.78, 128.83, 127.76, 127.45, 124.66, 124.60, 119.97, 119.66, 119.58, 119.21, 114.48, 114.43, 55.45, 55.42, 47.42, 36.99; MS (FAB) *m*/*z* 668.1 $(M+H)^+$; HRMS (FAB). Calcd for $C_{39}H_{34}O_4N_5S$: 668.2332. Found: 668.2379.

4.1.1.13. 2-(4-Phenyl-5-(2-phenylquinolin-4-yl)-4*H*-1,2,4-triazol-3-ylthio)-*N*-(4-((*E*)-3-(3,4,5-trimethoxyphenyl)acryloyl)phenyl)acetamide (9a).

Off-white solid (84%); m.p. 271-272 °C; IR (FT-IR, cm^{-1}): 3236 (NH), 1683 (C=O), 1655 (CO-NH); ^{1}H NMR (600 MHz, DMSO-d_6) δ (ppm): 10.87 (s, 1H, NH), 8.22 (d, *J* = 8.4 Hz, 2H, Ar-H), 8.14 (d, *J* = 8.4 Hz, 1H, Ar-H), 8.11 (d, *J* = 8.4 Hz, 1H, Ar-H), 8.07 (s, 1H, Ar-H), 8.04–8.02 (m, 2H, Ar-H), 7.92 (d, *J* = 15.6 Hz, 1H, $\underline{CH}$=CH), 7.85 (d, *J* = 8.4 Hz, 2H, Ar-H), 7.82–7.81 (m, 1H, Ar-H), 7.70 (d, *J* = 15.6 Hz, 1H, CH=$\underline{CH}$), 7.62 (t, *J* = 8.4 Hz, 1H, Ar-H), 7.54–7.50 (m, 5H, Ar-H), 7.48–7.44 (m, 3H, Ar-H), 7.25 (s, 2H, Ar-H), 4.40 (s, 2H, S-CH_2), 3.88 (s, 6H, 2-OCH_3), 3.73 (s, 3H, OCH_3); ^{13}C NMR (151 MHz, DMSO-d_6) δ (ppm): 187.98, 166.64, 155.68, 153.59, 152.55, 152.33, 148.31, 144.44, 143.62, 140.21, 138.25, 133.66, 133.61, 133.19, 130.99, 130.79, 130.53, 130.46, 130.27, 130.01, 129.40, 127.97, 127.81, 127.47, 126.02, 125.85, 125.00, 121.62, 120.88, 119.01, 107.02, 60.63, 56.65, 37.52; MS (FAB) *m*/*z* 734.4 $(M+H)^+$; HRMS (FAB). Calcd for $C_{43}H_{36}O_5N_5S$: 734.2437. Found: 734.2444.

4.1.1.14. 2-(4-Allyl-5-(2-phenylquinolin-4-yl)-4*H*-1,2,4-triazol-3-ylthio)-*N*-(4-((*E*)-3-(3,4,5-trimethoxyphenyl)acryloyl)phenyl)acetamide (9b).

Pale yellow solid (78%); m.p. 217-218 °C; IR (FT-IR, cm^{-1}): 3242 (NH), 1677 (C=O), 1659 (CO-NH); ^{1}H NMR (600 MHz, DMSO-d_6) δ (ppm): 10.82 (s, 1H, NH), 8.32–8.30 (m, 2H, Ar-H), 8.30

(s, 1H, Ar-H), 8.24–8.20 (m, 3H, Ar-H), 7.91 (d, *J* = 15.6 Hz, 1H, CH=CH), 7.89–7.86 (m, 2H, Ar-H), 7.84 (d, *J* = 9.0 Hz, 2H, Ar-H), 7.70 (d, *J* = 15.6 Hz, 1H, CH=CH), 7.63 (t, *J* = 7.8 Hz, 1H, Ar-H), 7.61–7.57 (m, 2H, Ar-H), 7.57–7.55 (m, 1H, Ar-H), 7.25 (s, 2H, Ar-H), 5.90–5.83 (m, 1H, CH_2-CH=CH_2), 5.13 (d, *J* = 10.4 Hz, 1H, -CH=CH_2), 4.84 (d, *J* = 17.4 Hz, 1H, -CH=CH_2), 4.65 (d, *J* = 4.8 Hz, 2H, CH_2-CH), 4.36 (s, 2H, S-CH_2), 3.88 (s, 6H, 2-OCH_3), 3.73 (s, 3H, OCH_3); ^{13}C NMR (151 MHz, DMSO-d_6) δ (ppm): 187.50, 166.33, 155.61, 153.11, 152.03, 151.12, 148.01, 143.96, 143.10, 139.73, 137.90, 133.64, 132.74, 132.14, 130.60, 130.30, 130.03, 129.98, 129.70, 128.94, 127.59, 127.29, 125.17, 124.83, 121.13, 119.65, 118.55, 117.52, 106.52, 60.13, 56.15, 46.71, 37.8; MS (FAB) *m*/*z* 698.4 $(M+H)^+$; HRMS (FAB). Calcd for $C_{40}H_{36}O_5N_5S$: 698.2437. Found: 698.2481.

4.1.1.15. 2-(5-(2-(4-Chlorophenyl)quinolin-4-yl)-4-phenyl-4*H*-1,2,4-triazol-3-ylthio)-*N*-(4-((*E*)-3-(3,4,5-trimethoxyphenyl)acryloyl)phenyl)acetamide (9c).

White solid (67%); m.p. 146-147 °C; IR (FT-IR, cm^{-1}): 3249 (NH), 1677 (C=O), 1659 (CO-NH); ^{1}H NMR (600 MHz, DMSO-d_6) δ (ppm): 10.85 (s, 1H, NH), 8.22 (d, *J* = 8.4 Hz, 2H, Ar-H), 8.12–8.08 (m, 5H, Ar-H), 7.92 (d, *J* = 15.6 Hz, 1H, CH=CH), 7.84 (d, *J* = 9.0 Hz, 2H, Ar-H), 7.83–7.81 (m, 1H, Ar-H), 7.70 (d, *J* = 15.6 Hz, 1H, CH=CH), 7.64 (t, *J* = 8.4 Hz, 1H, Ar-H), 7.60 (d, *J* = 9.0 Hz, 2H, Ar-H), 7.51 (d, *J* = 8.4 Hz, 2H, Ar-H), 7.46–7.42 (m, 3H, Ar-H), 7.25 (s, 2H, Ar-H), 4.41 (s, 2H, S-CH_2), 3.88 (s, 6H, 2-OCH_3), 3.73 (s, 3H, OCH_3);^{13}C NMR (151 MHz, DMSO-d_6) δ (ppm): 187.97, 166.62, 154.45, 153.60, 152.58, 152.28, 148.21, 144.44, 143.61, 140.23, 137.03, 135.45, 133.91, 133.54, 133.20, 131.13, 130.78, 130.55, 130.46, 130.25, 130.01, 129.47, 129.19, 128.18, 127.77, 126.00, 125.08, 121.61, 120.78, 119.01, 107.02, 60.62, 56.65, 37.51; MS (FAB) *m*/*z* 768.2 $(M+H)^+$; HRMS (FAB). Calcd for $C_{43}H_{35}O_5N_5ClS$: 768.2047. Found: 768.2043.

4.1.1.16. 2-(4-Allyl-5-(2-(4-chlorophenyl)quinolin-4-yl)-4*H*-1,2,4-triazol-3-ylthio)-*N*-(4-((*E*)-3-(3,4,5-trimethoxyphenyl)acryloyl)phenyl)acetamide (9d).

Pale yellow solid (76%); m.p. 234-235 ^{o}C; IR (FT-IR, cm^{-1}): 3244 (NH), 1676 (C=O), 1660 (CO-NH); ^{1}H NMR (600 MHz, DMSO-d_6) δ (ppm): 10.82 (s, 1H, NH), 8.34 (d, J = 9.0 Hz, 2H, Ar-H), 8.32 (s, 1H, Ar-H), 8.21 (t, J = 9.0 Hz, 3H, Ar-H), 7.91 (d, J = 15.6 Hz, 1H, CH=CH), 7.89–7.82 (m, 4H, Ar-H), 7.70 (d, J = 15.6 Hz, 1H, CH=CH), 7.67–7.63 (m, 3H, Ar-H), 7.24 (s, 2H, Ar-H), 5.88–5.81 (m, 1H, CH_2-CH=CH_2), 5.11 (d, J = 10.4 Hz, 2H, CH=CH_2), 4.84 (d, J = 17.4 Hz, 2H, CH=CH_2), 4.65 (d, J= 4.8 Hz, 2H, CH_2-CH), 4.36 (s, 2H, S-CH_2), 3.88 (s, 6H, 2- OCH_3), 3.73 (s, 3H, OCH_3); ^{13}C NMR (151 MHz, DMSO-d_6) δ (ppm): 187.50, 166.31, 154.42, 153.11, 151.93, 151.15, 147.93, 143.97, 143.09, 139.73, 136.71, 134.99, 133.83, 132.74, 132.10, 130.73, 130.29, 129.97, 129.69, 129.05, 128.98, 127.81, 125.18, 124.92, 121.12, 119.59, 118.54, 117.57, 106.52, 60.13, 56.15, 46.70, 37.79; MS (FAB) m/z 732.2 $(M+H)^+$; HRMS (FAB). Calcd for $C_{40}H_{35}O_5N_5ClS$: 732.2047. Found: 732.2072.

4.1.1.17. 2-(5-(2-(4-Methoxyphenyl)quinolin-4-yl)-4-phenyl-4*H*-1,2,4-triazol-3-ylthio)-*N*-(4-((*E*)-3-(3,4,5-trimethoxyphenyl)acryloyl)phenyl)acetamide (9e).

White solid (73%); m.p. 198-200 ^{o}C; IR (FT-IR, cm^{-1}): 3316 (NH), 1691 (C=O), 1659 (CO-NH); ^{1}H NMR (600 MHz, DMSO-d_6) δ (ppm): 10.89 (s, 1H, NH), 8.22 (d, J = 9.0 Hz, 2H, Ar-H), 8.09 (d, J = 8.4 Hz, 1H, Ar-H), 8.05 (d, J = 8.4 Hz, 1H, Ar-H), 8.02 (s, 1H, Ar-H), 8.01 (d, J = 9.0 Hz, 2H, Ar-H), 7.92 (d, J = 15.6 Hz, 1H, CH=CH), 7.85 (d, J = 9.0 Hz, 2H, Ar-H), 7.78 (t, J = 8.4 Hz, 1H, Ar-H), 7.70 (d, J = 15.6 Hz, 1H, CH=CH), 7.57 (t, J = 7.2 Hz, 1H, Ar-H), 7.52–7.51 (m, 2H, Ar-H), 7.46–7.42 (m, 3H, Ar-H), 7.24 (s, 2H, Ar-H), 7.07 (d, J = 9.0 Hz, 2H, Ar-H), 4.40 (s, 2H, S-CH_2), 3.88 (s, 6H, 2-OCH_3), 3.84 (s, 3H, OCH_3), 3.73 (s, 3H, OCH_3); ^{13}C NMR (151 MHz, DMSO-d_6) δ (ppm): 187.98, 166.65, 161.41, 155.36, 153.60, 152.47, 152.42, 148.30, 144.43,

143.64, 140.23, 133.62, 133.48, 133.19, 130.85, 130.79, 130.69, 130.51, 130.45, 130.24, 129.77, 128.95, 127.80, 127.47, 125.94, 124.68, 121.62, 120.49, 119.02, 114.81, 107.02, 60.63, 56.65, 55.83, 37.53; MS (FAB) *m*/*z* 764.0 $(M+H)^+$; HRMS (FAB). Calcd for $C_{44}H_{38}O_6N_5S$: 764.2543. Found: 764.2574.

4.1.1.18. 2-(4-Allyl-5-(2-(4-methoxyphenyl)quinolin-4-yl)-4*H*-1,2,4-triazol-3-ylthio)-*N*-(4-((*E*)-3-(3,4,5-trimethoxyphenyl)acryloyl)phenyl)acetamide (9f).

Off-white solid (76%); m.p. > 300 °C; IR (FT-IR, cm^{-1}): 3243 (NH), 1677 (C=O), 1660 (CO-NH); ^1H NMR (600 MHz, DMSO-d_6) δ (ppm): 11.04 (s, 1H, NH), 8.29 (d, *J* = 8.9 Hz, 2H, Ar-H), 8.27 (s, 1H, Ar-H), 8.21 (d, *J* = 8.4 Hz, 2H, Ar-H), 8.15 (d, *J* = 8.4 Hz, 1H, Ar-H), 7.91 (d, *J* = 15.6 Hz, 1H, CH=CH), 7.87 (d, *J* = 8.4 Hz, 2H, Ar-H), 7.82 (t, *J* = 8.4 Hz, 2H, Ar-H), 7.69 (d, *J* = 15.6 Hz, 1H, CH=CH), 7.58 (t, *J* = 8.4 Hz, 1H, Ar-H), 7.24 (s, 2H, Ar-H), 7.13 (d, *J* = 8.4 Hz, 2H, Ar-H), 5.89–5.82 (m, 1H, CH_2-CH-CH_2), 5.12 (d, *J* = 10.8 Hz, 1H, CH-CH_2), 4.83 (d, *J* = 16.8 Hz, 1H, CH-CH_2), 4.65 (d, *J* = 4.2 Hz, 2H, CH_2-CH), 4.36 (s, 2H, S-CH_2), 3.88 (s, 6H, 2-OCH_3), 3.86 (s, 3H, OCH_3), 3.73 (s, 3H, OCH_3); ^{13}C NMR (151 MHz, DMSO-d_6) δ (ppm): 187.57, 166.40, 160.98, 155.28, 153.10, 152.33, 152.11, 150.94, 147.99, 143.93, 143.18, 139.72, 133.49, 132.69, 132.14, 130.61, 130.49, 130.30, 129.96, 129.93, 129.44, 128.78, 121.17, 119.25, 119.10, 118.58, 117.48, 114.36, 106.52, 60.14, 60.03, 56.16, 55.70, 55.35; MS (FAB) *m*/*z* 750.1 $(M+Na)^+$; HRMS (FAB). Calcd for $C_{41}H_{37}O_6N_5SNa$: 750.2362. Found: 750.2407.

4.2. Biology

4.2.1. *Screening of antiproliferative activity by NCI*

The methodology of the NCI anticancer screening has been described in detail elsewhere (http://www.dtp.nci.nih.gov), [46].

4.2.2. Cytotoxic activity using MTT Assay and evaluation of IC_{50}

4.2.2.1. MTT assay

MTT assay was performed to investigate the effect of the synthesized compounds on the viability of mammary epithelial cells (MCF-10A) [47, 48]. **See Appendix A**.

4.2.2.2. Assay for antiproliferative effect

To explore the antiproliferative potential of compounds MTT assay was performed according to previously reported procedure [49, 50] using different cell lines. **See Appendix A**.

4.2.2.3. EGFR inhibitory assay

EGFR-TK assay was performed to evaluate the inhibitory potency of the most active compounds **IVc**, **IVf**, and **IVg** against EGFR [51]. **See Appendix A**

4.2.2.4. BRAF kinase assay

V^{600E} mutant BRAF kinase assay was performed to investigate the activity of compounds **IVc**, **IVf**, and **IVg** against $BRAF^{V600E}$ [52]. **See Appendix A**

4.2.2.5. Cell apoptosis assay

Apoptosis was determined by flow cytometry based on the Annexin-V-fluoresce in isothiocyanate (FITC) and propidium iodide (PI) staining kit (BD Pharmingen, San Diego, USA) [53, 54]. **See Appendix A**.

4.3. Molecular docking

AutoDock 4.2 [40] was used to perform the docking study of the new compounds into the active site of EGFR and $BRAF^{V600E}$. The crystal structure of the two proteins, EGFR (pdb code: 1M17) [38] and $BRAF^{V600E}$ (pdb code: 3OG7) [39] were obtained from the Protein Data Bank (https://www.rcsb.org/structure). The chemical structure of the ligand and protein molecules were prepared according to the previous reports [41, 42]. The of grid and docking parameter files were prepared done by AutoDock tools (ADT) following the previous reports [43, 44]. Discovery Studio Visualizer [45] was used to generate the 3D binding modes of the new compounds into the two kinases. The results of the docking study were presented in Table **4**, Fig. **3-5** and in supplementary data (**Figs. S1-8**).

References

[1] R.L. Siegel, K.D. Miller, A. Jemal, Cancer statistics, 2019, CA. Cancer J. Clin. 69 (2019) 7–34.

[2] L.A. Torre, F. Bray, R.L. Siegel, J. Ferlay, J. Lortet-Tieulent, A. Jemal, Global cancer statistics, 2012, CA. Cancer J. Clin. 65 (2015) 87–108.

[3] A.S. Ibrahim, H.M. Khaled, N.N. Mikhail, H. Baraka, H. Kamel, Cancer Incidence in Egypt: Results of the National Population-Based Cancer Registry Program, J. Cancer Epidemiol. 2014 (2014) 1–18.

[4] S.H. Abbas, A.A. Abd El-Hafeez, M.E. Shoman, M.M. Montano, H.A. Hassan, New quinoline/chalcone hybrids as anti-cancer agents: Design, synthesis, and evaluations of cytotoxicity and PI3K inhibitory activity, Bioorganic Chem. 82 (2019) 360–377.

[5] C.S. Manohar, A. Manikandan, P. Sridhar, A. Sivakumar, B. Siva Kumar, S.R. Reddy, Drug repurposing of novel quinoline acetohydrazide derivatives as potent COX-2 inhibitors and anti-cancer agents, J. Mol. Struct. 1154 (2018) 437–444.

[6] R. Musiol, An overview of quinoline as a privileged scaffold in cancer drug discovery, Expert Opin. Drug Discov. 12 (2017) 583–597.

[7] A.M. Mohassab, H.A. Hassan, D. Abdelhamid, M. Abdel-Aziz, K.N. Dalby, T.S. Kaoud, Novel quinoline incorporating 1,2,4-triazole/oxime hybrids: Synthesis, molecular docking, anti-inflammatory, COX inhibition, ulceroginicity and histopathological investigations, Bioorganic Chem. 75 (2017) 242–259.

[8] K. Douadi, S. Chafaa, T. Douadi, M. Al-Noaimi, I. Kaabi, Azoimine quinoline derivatives: Synthesis, classical and electrochemical evaluation of antioxidant, anti-inflammatory, antimicrobial activities and the DNA / BSA binding, J. Mol. Struct. (2020) 128305.

[9] R. Musiol, Quinoline-based HIV integrase inhibitors, Curr. Pharm. Des. 19 (2013) 1835–1849.

[10] R.S. Keri, S.A. Patil, Quinoline: A promising antitubercular target, Biomed. Pharmacother. 68 (2014) 1161–1175.

[11] M.C. Joshi, T.J. Egan, Quinoline Containing Side-chain Antimalarial Analogs: Recent Advances and Therapeutic Application, Curr. Top. Med. Chem. 20 (2020) 617–697.

[12] C.A. Costa, R.M. Lopes, L.S. Ferraz, G.N.N. Esteves, J.F. Di Iorio, A.A. Souza, I.M. de Oliveira, F. Manarin, W.A.S. Judice, H.A. Stefani, T. Rodrigues, Cytotoxicity of 4-substituted quinoline derivatives: Anticancer and antileishmanial potential, Bioorg. Med. Chem. 28 (2020) 115511.

[13] K.D. Upadhyay, A.K. Shah, Evaluation of Pyrano[3,2 C] Quinoline Analogues as Anticancer Agents, Anticancer Agents Med. Chem. 19 (2019) 1285–1292.

[14] S. Jain, V. Chandra, P. Kumar Jain, K. Pathak, D. Pathak, A. Vaidya, Comprehensive review on current developments of quinoline-based anticancer agents, Arab. J. Chem. 12 (2019) 4920–4946.

[15] Ş.G. Küçükgüzel, P. Çıkla-Süzgün, Recent advances bioactive 1,2,4-triazole-3-thiones, Eur. J. Med. Chem. 97 (2015) 830–870.

[16] M.S. Malik, S.A. Ahmed, I.I. Althagafi, M.A. Ansari, A. Kamal, Application of triazoles as bioisosteres and linkers in the development of microtubule targeting agents, RSC Med. Chem. 11 (2020) 327–348.

[17] M. Gilandoust, K.B. Harsha, C.D. Mohan, A.R. Raquib, S. Rangappa, V. Pandey, P.E. Lobie, Basappa, K.S. Rangappa, Synthesis, characterization and cytotoxicity studies of 1,2,3-triazoles and 1,2,4-triazolo [1,5-a] pyrimidines in human breast cancer cells, Bioorg. Med. Chem. Lett. 28 (2018) 2314–2319.

[18] R. Paprocka, M. Wiese, A. Eljaszewicz, A. Helmin-Basa, A. Gzella, B. Modzelewska-Banachiewicz, J. Michalkiewicz, Synthesis and anti-inflammatory activity of new 1,2,4-triazole derivatives, Bioorg. Med. Chem. Lett. 25 (2015) 2664–2667.

[19] S. Eswaran, A.V. Adhikari, N.S. Shetty, Synthesis and antimicrobial activities of novel quinoline derivatives carrying 1,2,4-triazole moiety, Eur. J. Med. Chem. 44 (2009) 4637–4647.

[20] A. Thakur, P.S. Gupta, P. kumar shukla, A. verma, P. Pathak, 1, 2, 4-Triazole Scafolds : Recent Advances and Pharmacological Applications, Int. J. Curr. Res. Acad. Rev. 4 (2016) 277–296.

[21] R. Kharb, M. Shahar Yar, P.C. Sharma, Recent advances and future perspectives of triazole analogs as promising antiviral agents, Mini Rev. Med. Chem. 11 (2011) 84–96.

[22] V.K. Kamboj, P.K. Verma, A. Dhanda, S. Ranjan, 1,2,4-triazole derivatives as potential scaffold for anticonvulsant activity, Cent. Nerv. Syst. Agents Med. Chem. 15 (2015) 17–22.

[23] Z. Nowakowska, A review of anti-infective and anti-inflammatory chalcones, Eur. J. Med. Chem. 42 (2007) 125–137.

[24] S. Park, E.H. Kim, J. Kim, S.H. Kim, I. Kim, Biological evaluation of indolizine-chalcone hybrids as new anticancer agents, Eur. J. Med. Chem. 144 (2018) 435–443.

[25] F.F. Ahmed, A.A. Abd El-Hafeez, S.H. Abbas, D. Abdelhamid, M. Abdel-Aziz, New 1,2,4-triazole-Chalcone hybrids induce Caspase-3 dependent apoptosis in A549 human lung adenocarcinoma cells, Eur. J. Med. Chem. 151 (2018) 705–722.

[26] C. Karthikeyan, N.S.H. Narayana Moorthy, S. Ramasamy, U. Vanam, E. Manivannan, D. Karunagaran, P. Trivedi, Advances in Chalcones with Anticancer Activities, Recent Patents Anticancer Drug Discov. 10 (2014) 97–115.

[27] Y.-Q. Hu, C. Gao, S. Zhang, L. Xu, Z. Xu, L.-S. Feng, X. Wu, F. Zhao, Quinoline hybrids and their antiplasmodial and antimalarial activities, Eur. J. Med. Chem. 139 (2017) 22–47.

[28] Shaveta, S. Mishra, P. Singh, Hybrid molecules: The privileged scaffolds for various pharmaceuticals, Eur. J. Med. Chem. 124 (2016) 500–536.

[29] W.-B. Kuang, R.-Z. Huang, J.-L. Qin, X. Lu, Q.-P. Qin, B.-Q. Zou, Z.-F. Chen, H. Liang, Y. Zhang, Design, synthesis and pharmacological evaluation of new 3-(1H-benzimidazol-2-yl)quinolin-2(1H)-one derivatives as potential antitumor agents, Eur. J. Med. Chem. 157 (2018) 139–150.

[30] T.S. Kaoud, A.M. Mohassab, H.A. Hassan, C. Yan, S.X. Van Ravenstein, D. Abdelhamid, K.N. Dalby, M. Abdel-Aziz, NO-releasing STAT3 inhibitors suppress BRAF-mutant melanoma growth, Eur. J. Med. Chem. 186 (2020) 111885.

[31] H. Kumar, A. Chattopadhyay, R. Prasath, V. Devaraji, R. Joshi, P. Bhavana, P. Saini, S.K. Ghosh, Design, Synthesis, Physicochemical Studies, Solvation, and DNA Damage of Quinoline-

Appended Chalcone Derivative: Comprehensive Spectroscopic Approach toward Drug Discovery, J. Phys. Chem. B. 118 (2014) 7257–7266.

[32] C.-H. Tseng, Y.-L. Chen, C.-Y. Hsu, T.-C. Chen, C.-M. Cheng, H.-C. Tso, Y.-J. Lu, C.-C. Tzeng, Synthesis and antiproliferative evaluation of 3-phenylquinolinylchalcone derivatives against non-small cell lung cancers and breast cancers, Eur. J. Med. Chem. 59 (2013) 274–282.

[33] G.C. Muscia, J.P. Carnevale, M. Bollini, S.E. Asis, Microwave-assisted döbner synthesis of 2-phenylquinoline-4-carboxylic acids and their antiparasitic activities, J. Heterocycl. Chem. 45 (2008) 611–614.

[34] Z. Xu, P. Xi, F. Chen, X. Liu, Z. Zeng, Synthesis, characterization, and DNA-binding properties of copper(II), cobalt(II), and nickel(II) complexes with salicylaldehyde 2-phenylquinoline-4-carboylhydrazone, Transit. Met. Chem. 33 (2007) 267–273.

[35] Z.H. Xu, P.X. Xi, F.J. Chen, Z.Z. Zeng, Synthesis, characterization, and DNA-binding of Ln(III) complexes with 2-hydroxybenzylidene-2-phenylquinoline-4-carbonylhydrazone, J. Coord. Chem. 62 (2009) 2193–2202.

[36] H.A.A. El-Aal, T.I. El-Emary, Efficient synthesis, characterization and biological evaluation of some new atophan carbohydrazide derivatives, J. Chem. Pharm. Res. 6 (2014) 90–99.

[37] F.F. Ahmed, A.A. Abd El-Hafeez, S.H. Abbas, D. Abdelhamid, M. Abdel-Aziz, New 1,2,4-triazole-Chalcone hybrids induce Caspase-3 dependent apoptosis in A549 human lung adenocarcinoma cells, Eur. J. Med. Chem. 151 (2018) 705–722.

[38] J. Stamos, M.X. Sliwkowski, C. Eigenbrot, Structure of the epidermal growth factor receptor kinase domain alone and in complex with a 4-anilinoquinazoline inhibitor, J. Biol. Chem. 277 (2002) 46265–46272.

[39] G. Bollag, P. Hirth, J. Tsai, J. Zhang, P.N. Ibrahim, H. Cho, W. Spevak, C. Zhang, Y. Zhang, G. Habets, E.A. Burton, B. Wong, G. Tsang, B.L. West, B. Powell, R. Shellooe, A. Marimuthu, H. Nguyen, K.Y.J. Zhang, D.R. Artis, J. Schlessinger, F. Su, B. Higgins, R. Iyer, K. D'Andrea, A. Koehler, M. Stumm, P.S. Lin, R.J. Lee, J. Grippo, I. Puzanov, K.B. Kim, A. Ribas, G.A. McArthur, J.A. Sosman, P.B. Chapman, K.T. Flaherty, X. Xu, K.L. Nathanson, K. Nolop,

Clinical efficacy of a RAF inhibitor needs broad target blockade in BRAF-mutant melanoma., Nature. 467 (2010) 596–599.

[40] G.M. Morris, R. Huey, W. Lindstrom, M.F. Sanner, R.K. Belew, D.S. Goodsell, A.J. Olson, AutoDock4 and AutoDockTools4: Automated docking with selective receptor flexibility, J. Comput. Chem. 30 (2009) 2785–2791.

[41] A.M. Gouda, F.A. Almalki, Carprofen: a theoretical mechanistic study to investigate the impact of hydrophobic interactions of alkyl groups on modulation of COX - 1/2 binding selectivity, SN Appl. Sci. 1 (2019) 1-15.

[42] T.S. Ibrahim, R.M. Bokhtia, A.M.M. AL-Mahmoudy, E.S. Taher, M.A. AlAwadh, M. Elagawany, E.H. Abdel-Aal, S. Panda, A.M. Gouda, H.Z. Asfour, N.A. Alhakamy, B.G.M. Youssif, Design, synthesis and biological evaluation of novel 5-((substituted quinolin-3-yl/1-naphthyl) methylene)-3-substituted imidazolidin-2,4-dione as HIV-1 fusion inhibitors, Bioorg. Chem. 99 (2020) 103782.

[43] M.S. Shaykoon, A.A. Marzouk, O.M. Soltan, A.S. Wanas, M.M. Radwan, A.M. Gouda, B.G.M. Youssif, M. Abdel-Aziz, Design, synthesis and antitrypanosomal activity of heteroaryl-based 1,2,4-triazole and 1,3,4-oxadiazole derivatives, Bioorg. Chem. 100 (2020) 103933.

[44] K.M. Attalah, A.N. Abdalla, A. Aslam, M. Ahmed, M.A.S. Abourehab, N.A. ElSawy, A.M. Gouda, Ethyl benzoate bearing pyrrolizine/indolizine moieties: Design, synthesis and biological evaluation of anti-inflammatory and cytotoxic activities, Bioorg. Chem. 94 (2020) 103371.

[45] Dassault systems BIOVIA, Discovery Studio Visualizer, v16.1.0.15350, San Diego: Dassault systems, (2016).

[46] H.A.M. El-Sherief, B.G.M. Youssif, S.N.A. Bukhari, M. Abdel-Aziz, H.M. Abdel-Rahman, Novel 1,2,4-triazole derivatives as potential anticancer agents: Design, synthesis, molecular docking, and mechanistic studies., Bioorg. Chem. 76 (2018) 314–325.

[47] H.-L. Qin, J. Leng, B.G.M. Youssif, M.W. Amjad, M.A.G. Raja, M.A. Hussain, Z. Hussain, S.N. Kazmi, S.N.A. Bukhari, Synthesis, and mechanistic studies of curcumin analog-based oximes as potential anticancer agents., Chem. Biol. Drug Des. 90 (2017) 443–449.

[48] B.G.M. Youssif, M.H. Abdelrahman, A.H. Abdelazeem, M.A. Abdelgawad, H.M. Ibrahim, O.I.A. Salem, M.F.A. Mohamed, L. Treambleau, S.N.A. Bukhari, Design, synthesis, mechanistic and histopathological studies of small-molecules of novel indole-2-carboxamides and pyrazino[1,2-a]indol-1(2H)-ones as potential anticancer agents effecting the reactive oxygen species production., Eur. J. Med. Chem. 146 (2018) 260–273.

[49] M. H. Abdelrahman, A. S. Aboraia, B. G. M. Youssif, B. E. M. Elsadek, Design, Synthesis and Pharmacophoric Model Building of New 3-Alkoxymethyl / 3-Phenyl indole-2-carboxamides with Potential Antiproliferative Activity, *Chem Biol Drug Des.* 90 (2017) 64-82.

[50] A.H. Abdelazeem, M.T. El-Saadi, E.G. Said, B.G.M. Youssif, H.A. Omar, S.M. El-Moghazy, Novel diphenylthiazole derivatives with multi-target mechanism: Synthesis, docking study, anticancer and anti-inflammatory activities., Bioorg. Chem. 75 (2017) 127–138.

[51] M. Hisham, B.G.M. Youssif, E.E.A. Osman, A.M. Hayallah, M. Abdel-Aziz, Synthesis, and biological evaluation of novel xanthine derivatives as potential apoptotic antitumor agents., Eur. J. Med. Chem. 176 (2019) 117–128.

[52] M.S. Abdelbaset, G.E.-D.A. Abuo-Rahma, M.H. Abdelrahman, M. Ramadan, B.G. Youssif, S.N.A. Bukhari, M.F. Mohamed, M. Abdel-Aziz, Novel pyrrol-2 (3*H*)-ones and pyridazin-3 (2*H*)-ones carrying quinoline scaffold as anti-proliferative tubulin polymerization inhibitors, Bioorg. Chem. 80 (2018) 151-163.

[53] B.G.M. Youssif, A.M. Mohamed, E.E.A. Osman, O.F. Abou-Ghadir, D.H. Elnaggar, M.H. Abdelrahman, L. Treamblu, H.A.M. Gomaa, 5-Chlorobenzofuran-2-carboxamides: From allosteric CB1 modulators to potential apoptotic antitumor agents, Eur. J. Med. Chem. 177 (2019) 1–11.

[54] H.A. Abou-Zied, B.G.M. Youssif, M.F.A. Mohamed, A.M. Hayallah, M. Abdel-Aziz, EGFR inhibitors and apoptotic inducers: Design, synthesis, anticancer activity, and docking studies of novel xanthine derivatives carrying chalcone moiety as hybrid molecules, Bioorg. Chem. 89 (2019) 102997.

Graphical Abstract

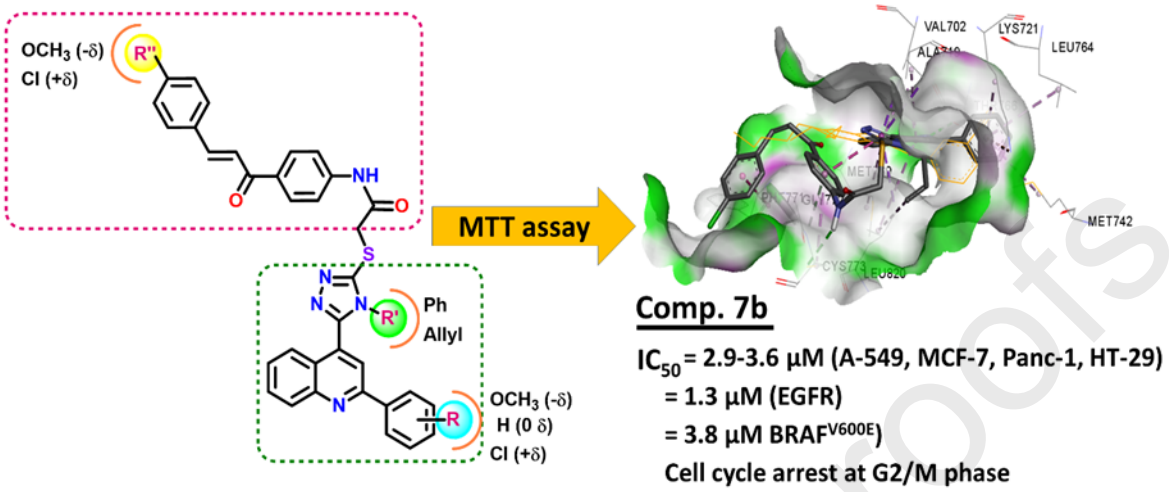

Highlights

- A series of quinoline/chalcone/1,2,4-triazole hybrids was synthesized and tested by NCI for their anticancer activity.
- **7b**, **7d**, **9b**, and **9d** were the most active compounds in most cancer cell lines with a growth inhibition between 77 and 94%.
- *In vitro* antiproliferative activity of the new hybrids was evaluated using MTT assay.
- Compounds **7a, 7b, 9a, 9b,** and **9d** showed promising antiproliferative activities and were evaluated against EGFR and $BRAF^{V600E}$.
- A docking study of compounds **7a, 7b, 9a, 9b, and 9d** showed good binding affinities towards EGFR and $BRAF^{V600E}$.

Conflicts of interest

The authors declare no conflict of interest